Progress in Polymer Science 165 (2025) 101967

Contents lists available at ScienceDirect

Progress in Polymer Science

journal homepage: www.elsevier.com/locate/progpolymsci

Baroplastics – The future of low temperature plastic processing☆

Daniel MacKinnon, Magdalena Godzina, C. Remzi Becer*

Department of Chemistry, University of Warwick, Coventry CV4 7AL, United Kingdom

ARTICLE INFO

Article history:
Received 27 September 2024
Revised 28 February 2025
Accepted 7 May 2025
Available online 11 May 2025

Keywords:
Baroplastic
Closed-loop
Sustainability
Polymer recycling

ABSTRACT

While global annual plastic production has surpassed 400 million tons, the rate of plastic recycling remains below 10 %. Recycling rates for conventional thermoplastics remain low, largely due to the harsh conditions required for high-temperature melt-molding. These conditions promote thermo-oxidative reactions and chain scission, causing significant deterioration of polymer chains and reducing the recyclability of these materials. Additionally, the sustainability of this process is compromised by its high energy demands and harmful environmental impacts. Baroplastics provide an alternative recycling pathway that involves the use of low-temperature processing under pressure; a novel class of sustainable polymers that leverages their unique pressure-responsive properties to enable recycling at markedly reduced energy consumption and CO_2 emissions. Baroplastics rely on order-to-disorder transitions (ODTs), typically of block copolymers (BCPs), that allow for a rheological transition from an ordered solid to a disordered liquid-like state that can flow and be molded. Once pressure is removed, the liquid-like state returns to its original solid form with no observed degradation of the polymeric chains. In this review, we introduce the concept of baroplastics and explore the mechanisms that underpin their distinctive ability to flow under pressure for sustainable recycling. We discuss the technological and environmental advantages of baromechanical recycling, the potential for future implementation within industry, and the use of baroplastics in nanocomposites and biological systems. Moreover, we have thoroughly reviewed the scope, modelling, and synthesis of baroplastic materials to produce a guide to this growing field.

1. Introduction

Plastics have become an integral part of every aspect of our daily lives and routines. Since their discovery over a century ago, the global economy has become largely dependent on the production and usage of plastics; sectors such as healthcare, construction, packaging, transport and food production are among the most responsible for mass plastic consumption [1]. Since then, we have successfully optimized and scaled global plastic production at a rate detrimental to the environment, with global plastic production increasing from 2 million metric tons in 1950 to 380 million metric tons in 2015 [2]. This has created significant challenges for recycling initiatives, primarily due to the economic advantage of virgin polymer production over recycled materials. The low cost of virgin polymer production, driven by factors such as cheap oil prices and economies of scale [3], has made it difficult for recycled plastics to compete economically [4]. As of 2015, the global production of primary plastics reached 407 million metric tons, with only about 10 % of all plastic ever produced having been recycled [2]. This disparity highlights the struggle of recycling schemes to keep pace with the increasing rate of plastic production. Consequently, a disparity in the development rates of synthesis and end-of-life (EoL) management of these materials arises; inadequate recycling techniques and infrastructure result in the accumulation of non-degradable and mismanaged plastic waste within the environment which causes ecological imbalances with visible consequences. Additional problems with the plastic life-cycle include their dependance on petrochemicals and significant carbon emissions, with the carbon footprint of plastics accounting for 4.5 % of global greenhouse gas (GHG) emissions as of 2015 [4]. Currently, it is almost certain that plastic pollution trends will both persist and worsen with time; by 2060 the amount of plastic waste generated is likely to triple and, without remediation, over 50 % is likely to become unmanageable and end up in our oceans [5].

Nevertheless, plastics remain the preferred choice for most industries owing to their low cost, durability, ease of processability, and versatile properties that can be tuned to specific needs [6].

☆ This manuscript is dedicated to the memory of late Prof. Dr. Metin H. Acar.

* Corresponding author.
E-mail address: remzibecer@warwick.ac.uk (C.R. Becer).

https://doi.org/10.1016/j.progpolymsci.2025.101967

List of abbreviations

AFM	Atomic Force Microscopy
ATRP	Atom-Transfer Radical Polymerization
BCP	Block Copolymer
CAN	Covalent Adaptable Network
CNT	Carbon Nanotubes
CSNPs	Core-Shell Nanoparticles
DA	Diels-Alder
DBCP	Diblock Copolymer
DSC	Dynamic Scanning Calorimetry
EMI SE	Electromagnetic Interference Shielding Efficiency
EoL	End-of-Life
EOS	Equation of State
EP	Emulsion Polymerization
FH	Flory-Huggins Regular Solution
FT-IR	Fourier Transform Infrared
GHG	Greenhouse Gas
GO	Graphene Oxide
h-BN	Hexagonal Boron Nitride
HDPE	High-Density Poly(ethylene)
LCST	Lower Critical Solution Temperature
LDOT	Lower Disorder-Order Transition
MAS	Magic Angle Spinning
MMT	Montemillonitrile
M_n	Number-average Molecular Weight
MW	Molecular Weight
M_w	Weight-average Molecular Weight
N	Polymer Chain length
n	# Carbons in monomer alkyl side chain
ODT	Order-Disorder Transition
P(dS)	Poly(deuterated styrene)
PAA	Poly(acrylic acid)
PBA	Poly(butyl acrylate)
PBMA	Poly(butyl methacrylate)
PBS	Poly(butylene succinate)
PCL	Poly(caprolactone)
PDLA	Poly(D-lactide)
PDXO	Poly(1,5-dioxepan-2-one)
PEA	Poly(ethyl acrylate)
PEHA	Poly(2-ethylhexyl acrylate)
PEMA	Poly(ethyl methacrylate)
PEO	Poly(ethylene oxide)
PHA	Poly(hydroxy alkanoates)
PHMA	Poly(hexyl methacrylate)
PIPP	Poly(2-Isopropoxy-2-oxo-1,3,2-dioxaphospholane)
PLA	Poly(lactide)
PLLA	Poly(L-lactide)
PLMA	Poly(lauryl methacrylate)
PmCL	Poly(caprolactone-r-5-ethylene ketal caprolactone)
PMMA	Poly(methyl methacrylate)
POMA	Poly(octyl methacrylate)
PP	Poly(propylene)
PPMA	Poly(propyl methacrylate)
PS	Poly(styrene)
PTMC	Poly(trimethylene carbonate)
P-V-T	Pressure, Volume, Temperature
r.t.	Room temperature
RGO	Reduced Graphene Oxide
ROP	Ring Opening Polymerization
SANS	Small Angle Neutron Scattering
SAXS	Small Angle X-Ray Scattering
SDGs	Sustainable Development Goals
SEBS	polystyrene-*b*-poly(ethylene-co-butylene)-*b*-polystyrene
SPN	Supramolecular Polymer Network
T_{ODT}	ODT Temperature
TBCP	Triblock Copolymer
TEM	Transmission Electron Microscopy
T_g	Glass Transition Temperature
$T_{g,hard}$	Hard Component Glass Transition Temperature
$T_{g,mix}$	Mixed-phase Glass Transition Temperature
$T_{g,soft}$	Soft Component Glass Transition Temperature
TMC	Trimethylene Carbonate
T_{proc}	Processing Temperature
UCST	Upper Critical Solution Temperature
UODT	Upper Order-Disorder Transition
UPy	Ureidopyrimidinone
w_{hard}	Mass fraction of hard component
w_{soft}	Mass fraction of soft component
δ	Solubility Parameter
ΔV_{mix}	Volume change on mixing
ρ_A	Density of polymer A
χ	Flory-Huggins Interaction Parameter
χ^{eff}	Effective Flory-Huggins Interaction Parameter

Rather than solely focusing on reducing plastic consumption, we must innovate new strategies to better manage our plastic waste that align with a circular plastics economy. This necessitates a systemic redesign of current EoL management approaches, as outlined previously in literature [7]. The urgency of this redesign is underscored by the United Nations Sustainable Development Goals (SDGs), particularly SDG 9; Industry, Innovation, and Infrastructure [8]. SDG 9 emphasizes the need for upgrading infrastructure and retrofitting industries to make them sustainable, with increased resource-use efficiency and greater adoption of clean and environmentally sound technologies. In response to these global imperatives, >120 countries have introduced regulatory or economic policies to improve waste management, promote recycling, and reduce the usage of certain plastics to curb plastic pollution, as of 2022 [9]. This is reflected by new regulations introduced by European institutions such as the Single Use Plastic ban [10], Circular Economy action Plan and Plastic Strategy [11,12], and the UK Plastic Packaging Tax on any plastic packaging that contains <30 % recycled plastic [13]. However, these legislative efforts, while crucial, are not sufficient on their own [9]. They must be complemented by technological innovations that address the fundamental challenges of plastic recycling and waste management. In a world where climate change has increasingly prevalent socio-environmental impacts, implementing a circular-economy approach to increase the sustainability of polymer usage and eliminate end-of-life plastics becomes a global research imperative. This is where novel materials like baroplastics come into play, offering a propitious pathway towards more sustainable plastic use with superior recycling, when compared to conventional thermoplastics [14–17].

Baroplastics, a class of polymers which can be processed with the application of pressure, instead of heat, are uniquely well-suited to closed-loop life-cycles, as their significantly elongated lifetimes result in a delayed need for disposal [14–24]. Critically, this would allow us to slow down the accumulation of plastic in the natural environment, providing a more sustainable, long-term solution to managing our plastic production and waste. Additionally, a more immediate advantage of baroplastics is their potential to sizably decrease energy consumption and CO_2 emissions in manufacturing and reprocessing [15,25,26]. Baroplastics rely on the order-disorder transitions (ODTs), typically of Block Copolymers (BCPs) or other microphase separated polymers such as core-shell

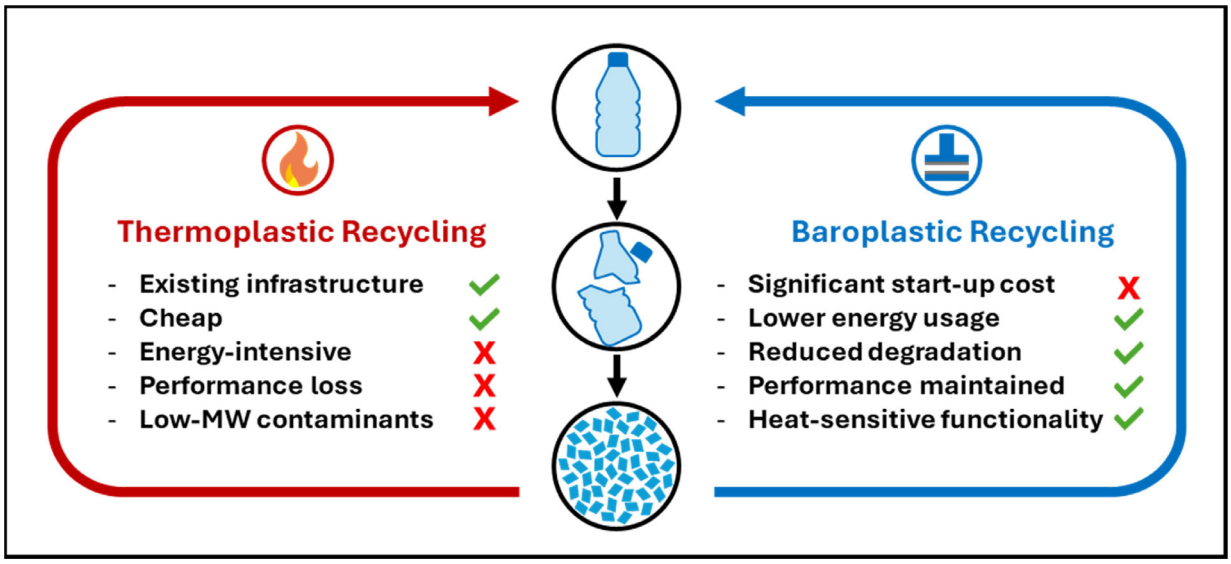

Fig. 1. An overview of both conventional thermoplastic and idealized baroplastic processing mechanisms, with some advantages and disadvantages given for each.

nanoparticles (CSNPs), that allow for a rheological transition from an ordered solid to a disordered liquid-like state that can flow and be molded. Under pressure, baroplastic materials exhibit an ODT and can be processed. Once pressure is removed, the liquid-like state returns to its original solid form with no observed degradation of the polymeric chains. This innovative class of sustainable polymers utilizes low processing temperatures (below 100 °C, often at ambient conditions), effectively preventing the degradation and oxidation of both the polymer and any incorporated compounds that would typically occur during conventional thermomechanical processing. Consequently, baromechanical recycling opens the door towards new applications; heat-sensitive molecules, such as proteins and drugs, can be incorporated within the material without the risk of their thermal inactivation upon manufacture and reprocessing [25–32]. Fig. 1 compares conventional thermoplastic recycling with baroplastic recycling, where baroplastic recycling benefits from lower energy costs, reduced material degradation leading to maintained performance over multiple processing cycles, and the ability to incorporate heat-sensitive functionalities.

In this review, we introduce the concept of baroplastics due to its novelty and complex theoretical background. We also highlight how we can leverage the pressure-responsive properties of these materials as we strive towards more sustainable global plastic recycling and management. There is a large potential scope for applications of these materials across numerous industries, as baroplastics offer versatile solutions for packaging, medical devices, consumer goods, automotive components, and more as we strive towards a global circular economy. While these materials are immediately of interest in somewhat niche applications, there is every possibility for the field to develop and provide genuinely circular replacements for large-scale commercial plastics such as thermoplastic elastomers.

2. Understanding baroplastics

The phenomenon of baroplastics has been explored [14,33–35], explained [19,22,24,36], and modelled [17,20,21], in great detail, previously. However, the complex nature of this topic may appear inaccessible to the wider polymer chemistry community, who otherwise might offer great contributions to the field. As such, a distilled history and explanation of baroplastic behavior is herein provided, in order to set in context, the content of the later sections of this review. The most significant developments, and some which will be discussed later in this review, are highlighted in Fig. 2.

2.1. High-temperature baroplastics

Polymer blends are often thermodynamically immiscible due to unfavorable enthalpic interactions, governed by a positive free energy of mixing (ΔG_{mix}) [37]. This leads to poor interfacial adhesion between polymers, often resulting in phase separation of the two chemically distinct domains [38], and similarly BCPs have the tendency to undergo microphase separation [39]. In both cases, these ordered phases can often be overcome, yielding a mixed, miscible phase, which typically occurs with increasing temperature. For polymer blends, these are termed Upper Critical Solution Temperatures (UCSTs), while for BCPs the term Upper Order-Disorder Transition (UODT) is used, which assumes the direction of increasing temperature. However, these terms essentially represent the same event, a mixing of two phase-separated polymer domains into a single phase. In the 1970s, a number of papers identified Lower Critical Solution Temperatures (LCSTs) in polymer blends, which differed from USCTs in that the system became ordered and phase-separated with increasing temperatures [40–42]. In a 1994 Nature paper, Russel et al. first reported the analogous lower critical ordering transition (also referred to as a Lower Disorder-Order Transition, LDOT) in a BCP, with a diblock copolymer (DBCP) of poly(deuterated styrene)-*b*-poly(butyl methacrylate) (PdS-*b*-PBMA) [18]. Unlike the conventional UODT, which was enthalpically driven, the microphase separation occurring at the LDOT was driven entropically by a negative volume change on the mixing of the two phases (ΔV_{mix}). Karis et al. studied this in greater detail by monitoring the variation of viscoelastic properties with frequency and temperature *via* rheology, finding the temperature of the LDOT to decrease linearly with increasing molecular weight (MW) [43]. Fig. 3 illustrates the range of different phase behaviors seen in BCPs/CSNPs through LDOT/UODT transitions and in polymer blends through analogous LCST/UCST transitions.

In 1998, Ruzette *et al.* extended the study to DBCPs of styrene and other *n*-alkyl methacrylates, finding that the phase behavior was dependent on the length of the alkyl methacrylate side chain (*n* carbons), specifically due to their varying compressible natures [35]. Equation of state parameters determined from literature group contribution calculations [44] and experimen-

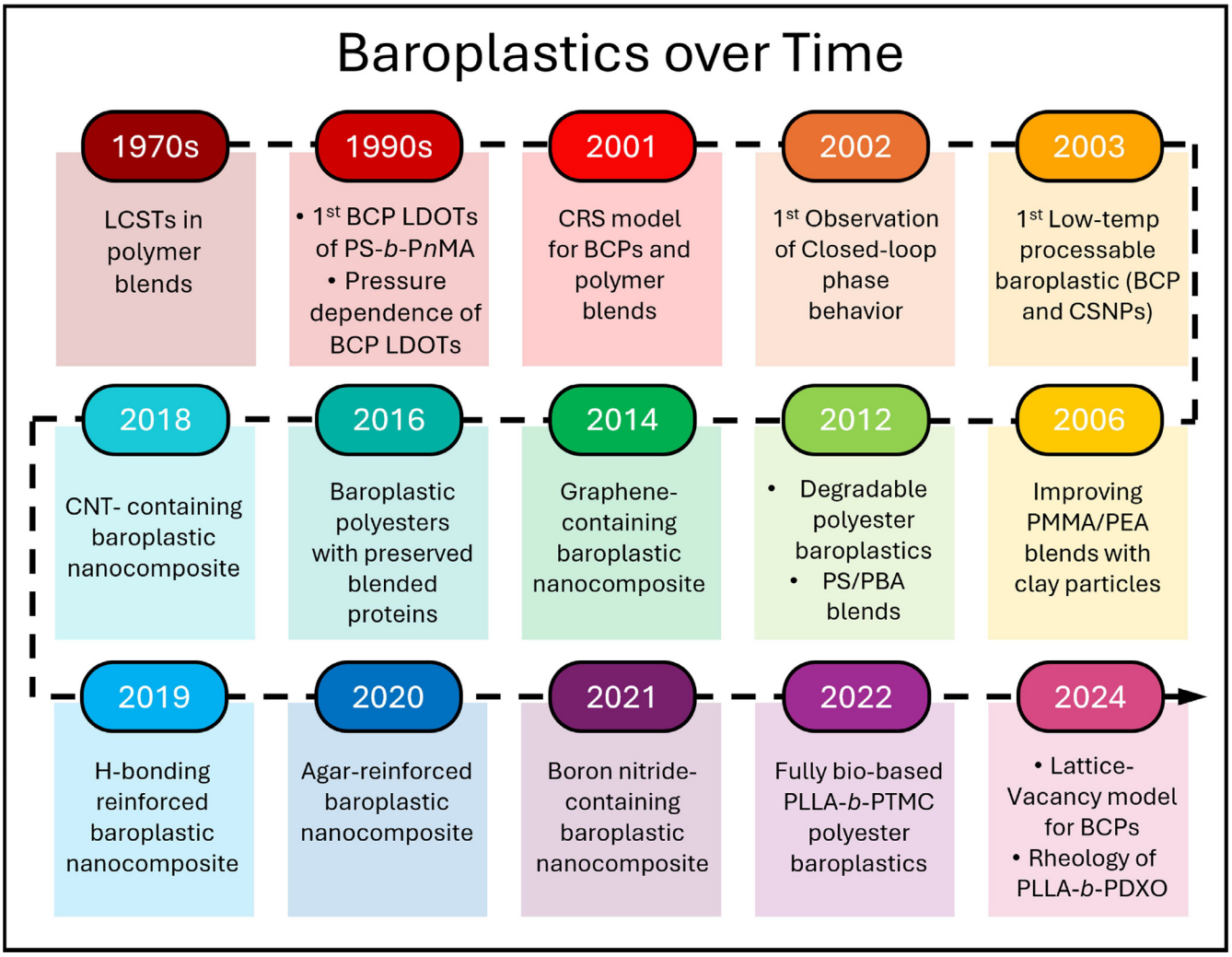

Fig. 2. A timeline of the development in the understanding and use of baroplastic materials, from the 1970s to 2025. LCST = Lower Critical Solution Temperature, BCP = Block Copolymer, LDOT = Lower Disorder-Order Transition, CRS = Compressible Regular Solution, CSNP = Core Shell Nanoparticles, CNT = Carbon Nanotubes.

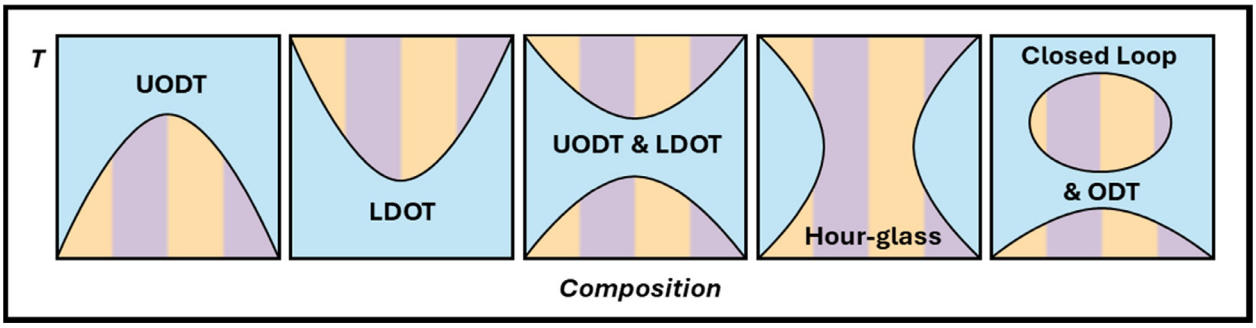

Fig. 3. A range of different phase behaviors seen in Block Copolymer (BCP) and Core-Shell Nanoparticle (CSNP) systems, based on Upper Order-Disorder Transitions (UODT) and Lower Disorder-Order Transitions (LDOT), where the striped region represents an ordered, phase-separated morphology, and the blue, shaded regions represent disordered, phase-mixed morphologies. In polymer blends, Upper Critical Solution Temperature (UCST) and Lower Critical Solution Temperature (LCST) behavior, analogous to UODT and LDOT behavior, respectively, can also be observed.

tal values [45,46] were used to determine Flory-Huggins interaction parameters (χ) for each polymer pair, which was directly related to the difference between the solubility parameters (δ_i) of each polymer (i) within the pair. The solubility parameter of the poly(n-alkyl methacrylate), δ_{nMA}, decreased from significantly greater than δ_{PS}(solubility parameter of poly(styrene)) when $n = 1$, to very similar to δ_{PS} when $n = 2$, 3, or 4, and finally to significantly lower than δ_{PS} when $n \geq 6$. As a result, DBCPs of PS with poly(methyl methacrylate) (PMMA), poly(hexyl methacrylate) (PHMA), poly(octyl methacrylate) (POMA), or poly(lauryl methacrylate) (PLMA) showed similar phase behavior, with an UODT and a weakly temperature-dependent χ. However, DBCPs of PS with poly(ethyl methacrylate) (PEMA), poly(propyl methacrylate) (PPMA), and poly(butyl methacrylate) (PBMA) showed an LDOT, with miscibility at lower temperature, and a transition towards an ordered state at an elevated temperature.

Interestingly, by combining PMMA and PLMA within the polymethacrylate block in such a ratio that the generated poly(methyl

methacrylate-co-lauryl methacrylate) P(MMA-*co*-LMA) copolymer has a specific volume and solubility parameter similar to that of PBMA, PS-*b*-P(MMA-*co*-LMA) exhibited LDOT behavior remarkably similar to that of PS-*b*-PBMA was observed [35]. As mentioned, LDOT ordering is entropically driven, with an increased number of configurations available after demixing, accompanied by an increase in volume. Under the application of high pressure, the denser, lower-volume, mixed phase is favored, resulting in a raised LDOT temperature [34,35,47,48]. For a DBCP of PS-*b*-PBMA under hydrostatic pressure, the LDOT temperature can increase by up to 1.47 °C MPa^{-1}; that is to say, a pressure increase of 10 MPa will increase the T_{LDOT} by almost 15 °C [34]. Hence, Ruzette et al. coined the term "Baroplastic", to describe a material which can flow and be processed under elevated pressures, at a temperature which is typically ordered, via the elevation of such an LDOT [35]. However, it is worth noting that these observations could only be made at significantly elevated temperatures, for which reason these materials are considered "High-Temperature Baroplastics".

The Flory-Huggins regular solution (FH) model, developed earlier [35,49–51], could describe the energy of mixing of two distinct weakly-interacting homopolymers, with the underlying assumptions that ΔV_{mix}=0 and that χ is purely enthalpic in nature. There are several major issues with the FH model, with two particularly relevant. Firstly, the effective interaction parameter (χ^{eff}) has been found to show temperature dependence due to an entropic component, which has, in some cases, accounted for more than half of the χ^{eff} value. Secondly, and most importantly, the FH model fails to predict the previously-observed LCST behavior of some polymer blends [20,42,52]. Both enthalpy and entropy changes must be positive for LCST-type phase behavior, which results from an increased entropy at high temperatures in the phase-separated state, relative to the mixed state [53]. This stands in contrast to the classical enthalpically-driven USCT [53]. Additionally, the ordering occurring at the LCST carries an implicit volume expansion, which explains the previously observed pressure dependence of LCSTs, with high pressures elevating the LCST due to preferring the denser miscible state [34,47,48]. UCST systems, however, can have either positive or negative ΔV_{mix}, and UCSTs can increase or decrease accordingly under high pressure [54,55] Prior to 2001, a number of equation-of-state (EOS) theories had been developed, extending the FH model to account for compressibility, such as the Flory, Orwoll, and Vrij modification of the general corresponding states [56,57], the lattice cluster theory [58], and the Sanchez-Lacombe lattice-fluid [53,59,60]. However, these more-rigorous models lacked predictive power, requiring experimental correction factors, which severely limited their usefulness in predicting phase diagrams.

From 2001 to 2003, a series of papers further developed the understanding of baroplastic behavior in both polymer blends and BCPs [14,19–24]. Ruzette et al. developed the Compressible Regular Solution (CRS) model, which qualitatively predicted the phase behavior of weakly interacting polymer pairs (Eq. (1)) [20,21].

$$\Delta G_{mix} = kT\left[\frac{\emptyset_A\tilde{\rho}_A}{N_A\nu_A}ln\emptyset_A + \frac{\emptyset_B\tilde{\rho}_B}{N_B\nu_B}ln\emptyset_B\right] + \emptyset_A\emptyset_B\tilde{\rho}_A\tilde{\rho}_B + \emptyset_A\emptyset_B(\tilde{\rho}_A - \tilde{\rho}_B)\left(\delta_A^2 + \delta_B^2\right) \quad (1)$$

Similar to the previously mentioned extensions of the FH model, the CRS model extended the FH model to account for thermal expansion and compressibility. The CRS model, however, was expressed in terms of pure component properties, without the need for experimental correction factors. Pure component properties were calculated from readily available pressure-volume-temperature (PVT) data [51,61], and group contribution calculations [62]. The first two terms of the CRS model are analogous to the FH terms of entropy and enthalpy of mixing, while the third term of the model accounts for compressibility; it is by far the most sensitive to pressure [21]. A positive third term indicates a positive ΔV_{mix}, while a negative third term indicates a negative ΔV_{mix}. It is this volume change which enables pressure to play a role.

To better understand this and its impact on baroplastic behavior, we can refer to EOS models, which are essential for analyzing compressibility differences between polymer components. The premise underpinning these models lies in the additional entropic factors, that can otherwise be deemed negligible for both polymer blends and BCPs. These dictate the free energy of mixing of these systems, potentially leading to destabilization, and hence phase separation, with elevated temperatures [20,21]. From a material design standpoint, understanding the PVT relationships that govern the thermodynamic entropic factors of these systems at a wide range of temperatures and pressures is extremely important as it allows us to predict behavior of systems [51]. While different EOS models vary in their ability to accurately predict polymer system behavior—particularly in relation to phase separation—most still rely on at least one interaction parameter derived from experimental data to achieve reliable phase behavior predictions. As a result, these models can provide a quantitative framework for assessing the variation in compressibility between polymer pairs, a key factor in the manifestation of baroplastic properties. This relationship with phase behavior was first qualitatively demonstrated for homopolymer blends of 23 weakly-interacting polymer pairs in 2001 by Mayes' group, through calculated spinodal phase diagrams correlating well with previously reported phase behaviors [21]. A simple free energy model, that was later coined the CRS model, was developed following the formalism typically adopted by EOS models. The studied blends were composed of PS, poly(methacrylate), poly(acrylate), poly(olefin), poly(carbonate), and poly(caprolactone) (PCL) homopolymers.

Comparison of the predicted UCST/LCST polymer blend behavior with the earlier-reported UODT/LDOT behavior of PS-poly(*n*-alkyl methacrylates) DBCPs showed good agreement, suggesting that the CRS model is also applicable to BCPs. However, one irregularity was observed in the predicted LCST behavior of a PS/PHMA blend [21], which contradicted the previously observed UODT behavior of a poly(styrene)-*b*-poly(hexyl methacrylate) (PS-*b*-PHMA) DBCP [35]. However, despite the observed UODT, PS-*b*-PHMA DBCPs were still expected to exhibit strong pressure effects, and this was then observed, with an unexpectedly large pressure coefficient of −0.6 °C MPa^{-1} determined [21]. Clearly, pressure had a much more significant effect than on most UODT-type BCPS, which typically exhibit smaller (and often positive) pressure coefficients of $< \pm 0.2$ °C MPa^{-1}. With specific reference to this large pressure coefficient and the large difference between the glass transition temperatures of the two blocks (105 °C), Ruzette et al. identified PS-*b*-PHMA as the first "baroplastics elastomer", a class of material which may exhibit processability at modest temperatures under high pressures [21]. In 2003, Ruzette et al. extended their pressure study of PS-poly(*n*-alkyl methacrylates) DBCPs, identifying the types of phase behavior (UODT/LDOT), the sign (±) of ΔV_{mix}, and the pressure coefficients of mixing (dT_{ODT}/dP) for each [22]. With intermediate-length alkyl side chains, packing is favorable for mixing at low temperatures, giving the LDOT behavior, while longer alkyl side chains suffer from unfavorable enthalpic interactions and lower packing efficiency in the mixed phase.

Two 2002 studies by Ryu *et al.* studied DBCPs [24], and polymer blends [23], of PS and poly(pentyl methacrylate) (PPMA); PS-*b*-PPMA and PS/PPMA, respectively. PS-*b*-PPMA showed closed-loop phase behavior for the first time in a weakly-interacting BCP system, where increasing temperature incurred an LDOT, and then a UODT, giving a closed-loop of microphase-separated material in an otherwise disordered phase diagram [24]. The phase behavior had a high MW dependency, with the UODT decreasing and the

LDOT increasing as MW decreased. In fact, at a number-average molecular weight value (M_n) of 48.7 kDa, the closed-loop behavior was observed, while at M_n = 46.5 kDa no microphase ordering occurred across the entire observed range. Within the small M_n window of 46.5–48.7 kDa, as the MW increased, the increasing LDOT met the decreasing UODT, creating the closed-loop seen in Fig. 3. In the same issue, Ruzette compared this discovery to the first-observed closed-loop systems, mixtures of nicotine in water [63], and suggested that very weak directional interactions may be sufficient to induce the disordering on cooling, giving LDOT behavior [19]. Furthermore, it was predicted that the behavior had only proved elusive thus-far due to the thermal degradation of polymers typically occurring prior to the mixing entropy becoming the dominant thermodynamic force [19]. An additional lower temperature ODT, below the LDOT, was theorized to exist, but as this would occur below the glass transition temperature (T_g) of the material, it could not be observed (Fig. 3) [24].

In the second study, PS/P*n*MA also showed a high dependency on MW, although the observed phase behavior was markedly different to that of the BCP [23]. When the MW of the PS homopolymer ($M_{n(PS)}$) was 6.6 kDa, a UCST, followed by an LCST, was observed with increasing temperature, with a wide miscible phase existing from 88–192 °C. On increasing $M_{n(PS)}$ to 7.1 kDa, the UCST increased and the LCST decreased until no mixed state was observed, giving an hourglass-shaped phase diagram. Closed-loop behavior, analogous to that of PS-*b*-PPMA, was thought to possibly arise at lower MW, but this incurred a UCST above the degradation temperature of 270 °C. Hence, lower-MW deuterium labelled PS (dPS) was used, which changed the UCST and LCST behavior due to the effect of the deuterium substitution [64]. The difference between the BCP and polymer blend behavior was attributed to differences in the temperature dependence of χ, although the reason for this disparity was not clearly identified, other than possibly small differences in the entropic contributions of blends and BCPs to χ values [23].

2.2. Low-temperature baroplastics

The most significant leap forward in baroplastic polymers came later in 2003, with the publication of the Nature paper "Low-Temperature Processing of 'Baroplastics' by Pressure-Induced Flow", by Gonzalez-Leon et al. [14] All prior baroplastic systems concerned ODTs at temperatures significantly above the T_g values of both components [18,19]. By combining a high- T_g and a low-T_g component, which showed miscibility under pressure, a flowing material could be induced at ambient temperatures [14]. It is noteworthy that this study, and all other subsequent works within the field, neglect to specify the nature of the pressure-responsive ODT as LDOT or UDOT. As such, the remainder of this review will, for the most part, simply refer to these transitions as ODTs. However, in all cases, the observed ODT spinodals match the appearance of UODT behavior, which is interesting as, of all the High-Temperature Baroplastics discussed in Section 2.1, only PS-*b*-PHMA displayed UODT behavior.

Suitable polymer combinations were identified using the CRS model, with the previously observed criterion for pressure-induced mixing that the densities of the two polymers should be close enough to one another that they are within 0.94 $\rho_A < \rho_B < 1.06\ \rho_A$ at 25 °C [35]. DBCPs of PS with poly(butyl acrylate) (PS-*b*-PBA) and with poly(2-ethylhexyl acrylate) (PS-*b*-PEHA), previously identified as potential baroplastic candidates by Mayes in 2001 [20,21], were able to be reprocessed under high pressure (34.5 MPa) at 25 °C into clear, well-defined extrudates and films [14]. A semi-solid partial mixing mechanism was identified *via* DSC analysis, which showed a retained glassy phase at 55 °C after processing. Notably, this work demonstrated how the T_g of each polymer in the baroplastic, both separate and combined, plays a significant role in a baroplastics ability to become processable under pressure at mild temperatures. Essentially, a high T_g "hard" segment is combined with a low T_g "soft" segment, which can be in the form of a polymer blend, BCP, or CSNP. The hard segment must have a T_g significantly above room temperature ($T_{g,\mathrm{hard}}$) to provide the material with rigidity and desirable mechanical properties under ambient conditions, while the soft segment has a lower T_g ($T_{g,soft}$). When pressure is applied, the temperature at which an ODT occurs (T_{ODT}) will be decreased. If two segments become (at least partially) miscible after passing through an ODT, a mixed phase will be generated, with a T_g value determined by the T_g (in K) and mass fractions (w) of the hard and soft segment ($T_{g,mix}$), according to the Fox equation (Eq. (2)).

$$\frac{1}{T_{g,\ mix}} = \frac{w_{hard}}{T_{g,hard}} + \frac{w_{soft}}{T_{g,\ soft}} \tag{2}$$

If $T_{g,mix}$ is below the processing temperature (T_{proc}), ideally below 25 °C, the material will behave as a viscous liquid, exhibiting low-temperature processability. Hence, the two prerequisites for low-temperature baroplastic flow in otherwise-suitable polymer pairs are 1) $T_{g,\ mix} > T_{ODT}$, and 2) $T_{g,\ mix} > T_{proc}$. Lowering $T_{g,soft}$ or increasing w_{soft} facilitates easier flow after passing the ODT, while also reducing the mechanical strength of the final material, with the inverse true for $T_{g,hard}$ and w_{hard}. [14] Typically, differential scanning calorimetry (DSC) is utilized to identify microphase separation at ambient pressure. In a microphase-separated polymeric structure, two distinct T_g's should be present on a DSC curve; this is indicative of the two separate immiscible polymer domains. However, exceptions to this criterion should be considered; factors such as incomplete phase-separation, proximal or overlapping T_g values, and T_g values with broad temperature ranges may result in DSC curves where two unambiguous domains cannot be clearly observed. After baroplastic processing, $T_{g,\ mix}$ is often also observed, due to some amount of mixed phase, generated during processing from the mixing of hard and soft domains, being retained afterwards. If only one T_g is present, the polymer is most-likely disordered at ambient pressure, with only a single mixed phase, and would therefore not be expected to exhibit baroplastic behavior. Interestingly, if mixing only occurs at the interfaces, the composition of the mixed phase may not reflect the true composition of the material, and $T_{g,mix}$ observed by DSC may not align with its predicted value, according to Eq. (2). Thus far, only PS, PMMA, and poly(L-lactide) (PLLA) have been utilized as hard segments, while a wide range of polyacrylate, polymethacrylate, and polyesters have been used as soft segments. Since 2003 and the first demonstration of low-temperature baroplastic behavior, a range of further baroplastics have been developed with varying polymer pairs, weight fractions, morphologies, as well as in several nanocomposites, and these will be the focus of the remainder of the review.

3. Classes of baroplastic

Due to the implicit requirement for a material capable of phase separation, baroplastic materials exist as one of the following: a polymer blend, a BCP, or CSNPs. In all cases, baroplastics comprise a mixture of hard and soft segments. Typically, a PS or PMMA segment is utilized for hard segments due to their low cost, high availability, and crucially, high T_g values, positioning them as ideal hard-segments in baroplastic materials. Contrastingly, the soft segments are often composed of a wider range of low T_g acrylate and methacrylate polymers. In this section, the three classes of baroplastics material based on styrenic, acrylate, and methacrylate polymers are discussed in detail. Notably, significant recent work on polyester and polycarbonate-based baroplastic BCPs has been conducted, which is discussed in Section 5. As illustrated in Fig. 4,

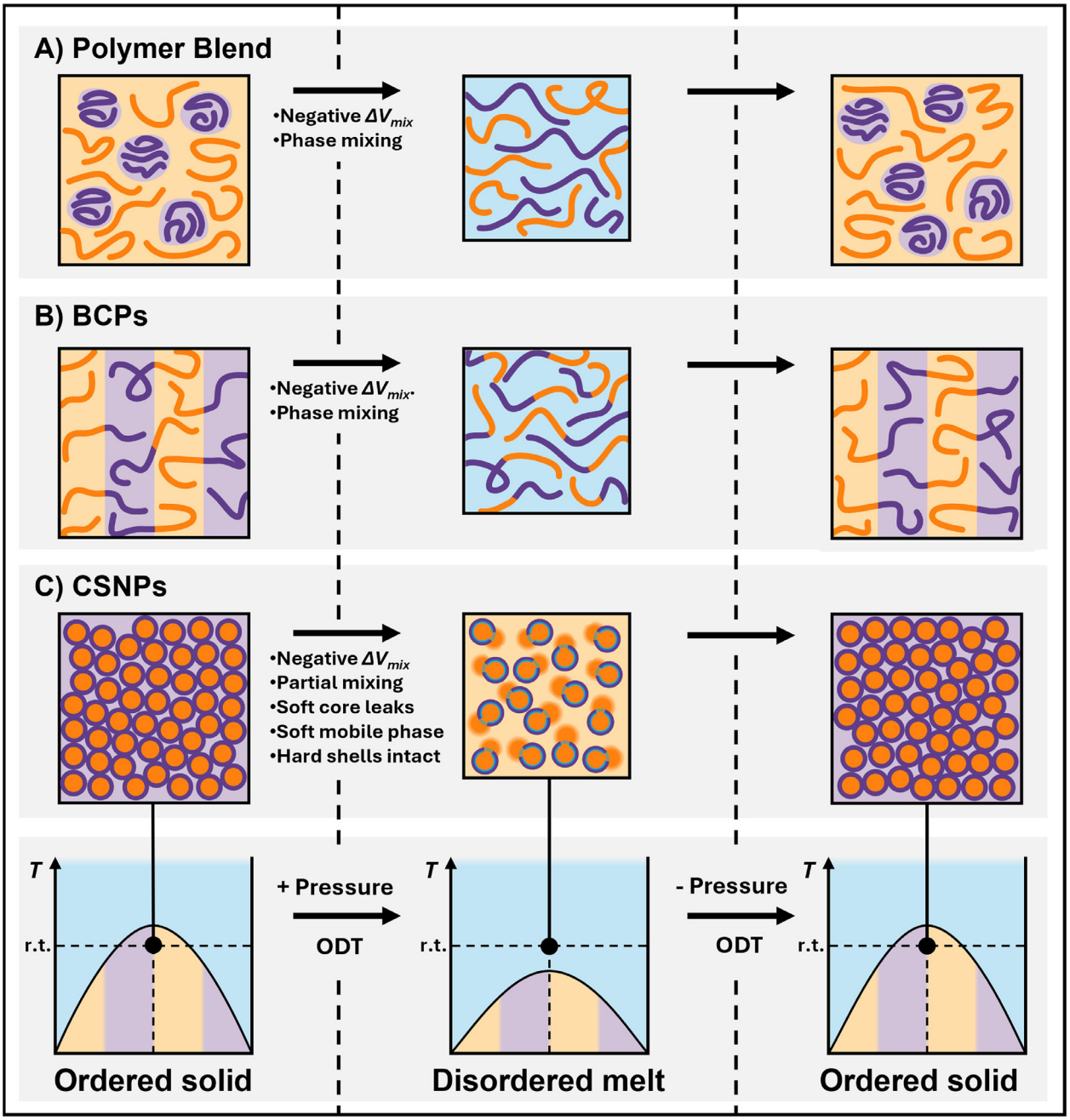

Fig. 4. A schematic demonstrating a baroplastic pressure-induced order-disorder transition (ODT) in **A)** a polymer blend, **B)** a Block Copolymer (BCP), and **C)** Core-Shell Nanoparticles (CSNPs), with the ODT spinodal shown to shift downwards under the application of pressure, due to a negative volume change on mixing (ΔV_{mix}), allowing the polymer to flow at ambient temperature.

the phase-separated hard and soft segments of a baroplastic determine whether a polymer blend, a BCP, or a CSNP, will show an ODT above room temperature (r.t.) with a negative ΔV_{mix}. As high pressures are applied, the denser mixed-phase is favored, depressing T_{ODT} to below r.t., at which point a mixed phase forms and can flow, until pressure is removed and the materials reverts back to phase-separation.

3.1. Polymer blends

A polymer blend (also known as nano- or poly- blends) is a mixture of two or more homopolymers that give rise to a new material with different properties. These are usually viscous solutions whose tendency to phase-separate depends on the chemical compatibility and MW of the homopolymers used, as both factors influence the entropy of mixing [33]. The different polymers within nano-blends are not chemically linked, providing a particularly simple method of combining the desirable thermal, mechanical, and physical properties of polymer materials in an economical way [65]. In particular, the effect of MW on the entropy of mixing can be modelled using the Flory-Huggins expression, which demonstrates that phase-separation is more likely to occur at higher MW and lower temperatures. However, it does not consider other crucial parameters such as differences in thermal expansion, compressibility and repeat unit size of the respective homopolymer component, which can drive de-mixing upon heating. Notably, phase-separation is often undesirable in polymer mixture as the large separate domains dramatically reduce the interfacial

Table 1
A summary of reported conventional styrenic, acrylic, and methacrylic-based baroplastic materials in the form of Polymer Blends (Hard/Soft) and Block Copolymers (BCPs)(Hard-*b*-Soft), prepared via Emulsion Polymerization (EP), Atom-Transfer Radical Polymerization (ATRP), or Anionic Polymerization.

Composition	*Polymer*						Processing			Ref.
(Hard/soft or hard-*b*-soft)	$T_{g,hard}$ [b] / °C	$T_{g,soft}$ [b] / °C	w_{hard} / wt%	M_n / kDa	$Đ$	Polym. Method	Temp / °C	Pressure / MPa	Time / min	
PMMA/PEA	105	−21	46	>200	2.0	EP	40	15	5	[32]
PMMA/PEA/MMT[a]	105	−21	46	>200	2.0	EP	40	15	5	[32]
PS/PBA	100	−53	62	469/400	2.73/ 2.45	EP	25	13.8	10	[72]
PS-*b*-PBA	100	−53	55	38	1,2	ATRP	25	34.5	5	[14]
PS-*b*-PEHA	100	−52	48	60	1,7	ATRP	25	34.5	5	[14]
PS-*b*-PPMA	100	−7	50	54	n.r.	Anionic	25	≈6.2	N/A	[73]
*d*PS-*b*-PPMA	100	−7	50	50	1.03	Anionic	90	5	N/A	[74]

[a] /MMT: compounded with montemillonitrile (MMT).
[b] Literature T_g values.

surface area between the polymer types, resulting in new materials with poor mechanical properties.

For this reason, numerous studies have focused on reducing incompatibility and improving material properties through the incorporation of compatibilizers and nanocomposites [31,65,66]. As most polymer mixtures show partial or full immiscibility within a working temperature range, the effect of temperature on the phase behavior of polymer blends has been extensively studied. There are two types of phase transitions reported in polymer blends; the UCST, which is the temperature above which two polymers can mix, and the LCST, which is the temperature above which two polymers phase-separate upon heating [67,68]. As mentioned earlier, these are directly analogous with the UODTs and LDOTs observed in BCPs, respectively.

The first study concerning baroplastic polymer blends was conducted by Xu et al. in 2006, who prepared a PMMA/PEA blend via emulsion polymerization, which could be processed at 15 MPa and 40 °C for 5 min into dogbone samples (**PMMA/PEA**, Table 1, Fig. 5**A.i**) [32]. Interestingly, DSC analysis after processing revealed a third transition at ≈ 45 °C, as well as the expected low and high glass transitions. This was suggested to be due to an increased interfacial region as a result of the pressure-induced miscibility causing the PEA phase to change from a co-continuous to a continuous morphology during processing. In 2012, Lee et al., demonstrated the baroplastic behavior of PS/PBA nanoblends, using a PS and poly-lauryl methacrylate (PLMA) nanoblend as a control [69]. They focused on the effect of increasing the hard-segment PS content on the properties of the material after processing at 13.8 MPa, 25 °C for ten minutes. Low PS content (w_{hard} < 42 wt%) resulted in opaque films which could not retain their shape when removed from their aluminum molds at room temperature due to their softness. Conversely, high PS content (w_{hard} > 83 wt%) yielded films which were semi-transparent and very brittle, likely due to the absence of a sufficiently-large soft segment to adhere the sample. In their system, the optimized PS content was identified as 62 wt%, which yielded the best-defined and mechanically strongest films (**PS/PBA**, Table 1, Fig. 5**A.ii**). Only two polymer blends have been reported as baroplastics, PS/PBA and PMMA/PBA, but both of these combinations have since been replicated within BCP and CSNP systems, as will be discussed in this review. Despite the challenges of avoiding macroscopic phase separation, the experimental simplicity of preparing polymer blends from simple homopolymers positions them well for the screening of baroplastic polymer pairs, even if any potential application would most-likely require the pair to be transferred to a CSNP or BCP system.

3.2. Block copolymers (BCPs)

BCPs are macromolecules comprised of two or more chemically distinct polymers covalently bonded together, which have been known to become ordered or disordered depending on temperature [18]. Depending on the degree of thermodynamic compatibility between the different blocks, such copolymers can either be segmentally mixed or microphase separated into microdomains consisting of the different block segments, with covalent junctions residing at the interface of each phase [70]. Naturally, chemically dissimilar polymers prefer to avoid one another due to intermolecular dispersion forces, but incompatible blocks are forced into close proximity in a BCP system [19]. At higher temperatures, entropy dominates, resulting in a disordered mixture, whereas when temperature drops, the system tries to combat the lower entropy through forming ordered microphase-separated structures. This manifests as a variety of morphologies, as shown in Fig. 6, determined by the weight fraction (and hence volume fraction) of each block, w_{hard} and w_{soft} [36]. Each morphology affects the mechanical properties of the copolymers in a different way, changing across the compositional range. The structures observed depend on several factors, including the MW of the blocks, the composition of the BCP and thermodynamic compatibility of the components (quantitatively depicted by the FH interaction parameter, χ) [71].

Since the first report in 2003, further DBCPs have been reported to exhibit low-temperature baroplastic behavior, which could provide a promising alternative to traditional thermal recycling methods. While research on baroplastics has been steadily progressing since the early 2000s, the rate of publications has notably increased in the last few years, primarily focusing on baroplastic BCPs. BCPs can show ODTs in the form of LDOTs and UODTs, analogous to the LCST and UCST transitions of polymer blends, respectively. Baroplastic BCPs are known to show ODTs at reduced temperatures, and in some cases at room temperature, under the application of high pressures, due to the depression of an ODT to below T_{proc}. Importantly, not all BCPs exhibit baroplastic behavior, as they must adhere to specific criteria which facilitates them undergoing pressure-responsive ODTs [14,22]. Additionally, as with the baroplastic polymer blends discussed in the previous section, such BCPs must have “hard” high- T_g segments and “soft” low- T_g segments [14,12].

As discussed earlier in this review, the first-reported mechanically processed baroplastic BCPs, poly(styrene)-*b*-poly(butyl acrylate) (PS-*b*-PBA) and poly(styrene)-*b*-poly(2-ethylhexyl acrylate) (PS-*b*-PEHA) DBCPs were synthesized by Gonzalez-Leon et al. via ATRP (**PS-*b*-PBA & PS-*b*-PEHA**, Table 1, Fig. 5**Bi-ii**) [14]. While prior baroplastic BCPs were proven using Small-Angle Neutron Scattering (SANS) at temperatures far above the T_g of both segments, these polymers could be processed in aluminum molds at room temperature. The two systems were initially demonstrated to be compatible by Ruzette [71]. In this work an additional criterion for pressure induced miscibility was identified; the densities of the two polymers, ρ_A and ρ_B, should be close enough to one another such that $0.94\ \rho_A < \rho_B < 1.06\ \rho_A$ at 25 °C [14]. M_n values for the three PS-*b*-PBA DBCPs were 100, 73, and 38 kDa, with 70, 63, and 55 wt% of PS, respectively. The PS-*b*-PEHA DBCP had

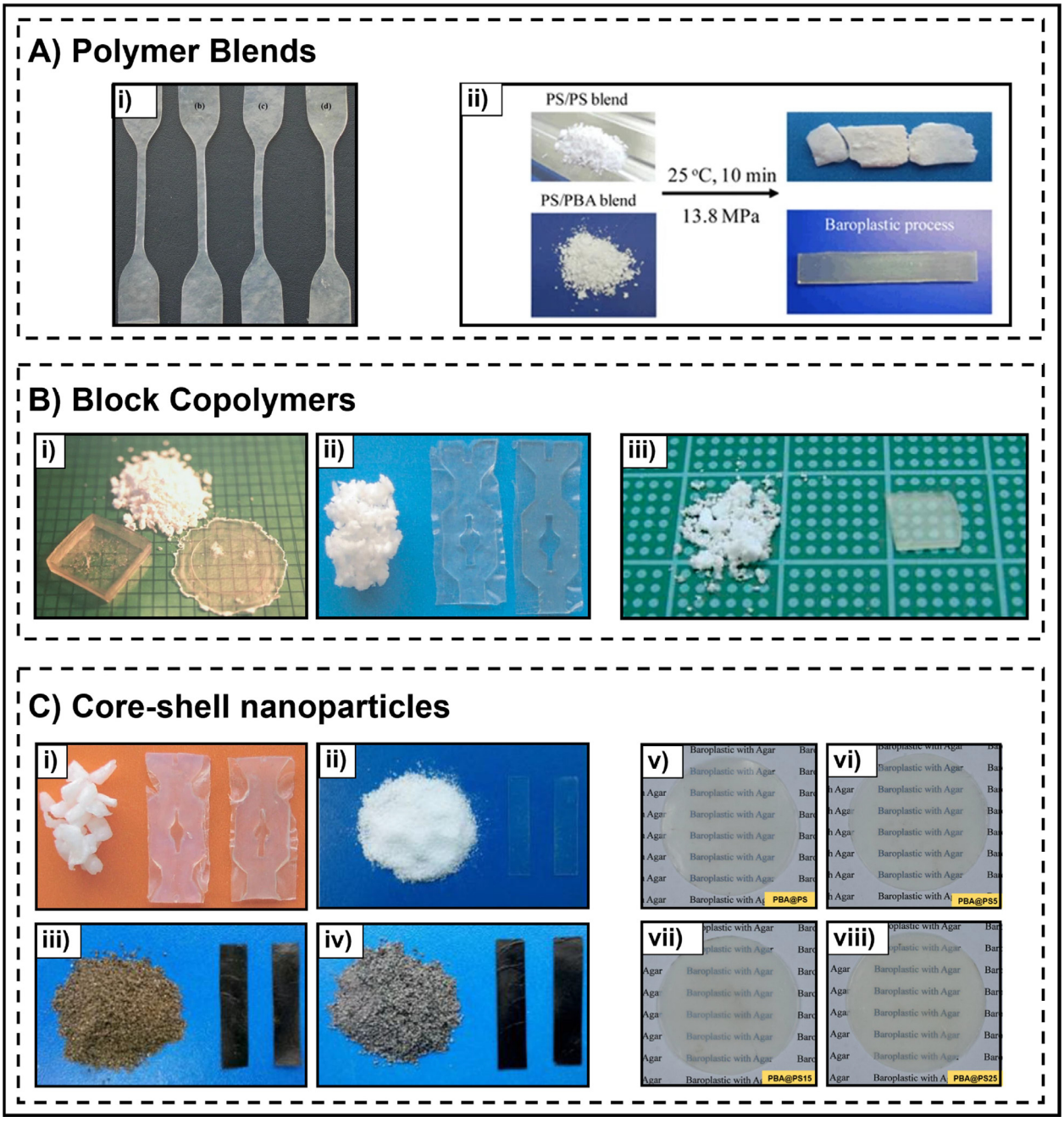

Fig. 5. Examples of literature baroplastics, before and after processing. A) Polymer blends: i) A PMMA/PEA blend with incorporated clay platelets could be processed into dog-bone shapes. ([32]. Copyright 2006. Adapted with permission from Elsevier Science Ltd.) ii) A PS/PS control blend showed poor processability, while iii) a PS/PBA blend could be processed under pressure to give a clear film. ([69]. Copyright 2012. Adapted with permission from Springer Publishing). B) Block Copolymers (BCPs): i) A PS-*b*-PBA DBCP, ii) a PS-*b*-PEHA DBCP ([14]. Copyright 2003. Adapted with permission from Springer Publishing), and iii) a PLLA-*b*-PmCL DBCP before and after baroplastic reprocessing. ([16]. Copyright 2012. Adapted with permission from American Chemical Society. C) Core-shell Nanoparticles (CSNPs): i) PS/PBA CSNPs ([14]. Copyright 2003. Adapted with permission from Springer Publishing), ii) PMMA/PBA CSNPs, and nanocomposites of PMMA/PBA CSNPs with iii) graphene oxide and iv) reduced graphene oxide, before and after baroplastic reprocessing ([31]. Copyright 2014. Adapted with permission from Institute of Physics Publishing Ltd.), and v-viii) reprocessed PS/PBA CSNPs nanocomposites with varying amounts of agar. ([26]. Copyright 2020. Adapted with permission from the American Chemical Society.).

a M_n of 60 kDa and a w_{hard} of 48 wt%. In most cases, the DBCPs were successfully processed at ambient temperature and yielded rigid, well-defined, clear extrudates and films, although the PS-*b*-PBS DBCP with a w_{hard} of 70 wt% required 80 °C and 34.5 MPa to be successfully reprocessed. Processed DBCPs could be shredded and reprocessed ten times with no apparent physical or mechanical degradation to the polymer. As seems intuitive, increasing w_{hard} reduced the ability of the material to undergo baroplastic flow and increased the $T_{g,mix}$, such that a higher temperature was required for processing. Importantly, 80 °C is still significantly below the 100 °C $T_{g,\ hard}$ for PS, so clearly the material is still behaving as a baroplastic. This highlights that, although low-temperature (i.e. near-ambient) processing is desirable, there may be opportunities to achieve materials with great mechanical properties by processing with mild heating (below 100 °C). Importantly, this must be considered alongside both the energy usage required to heat the material, and the temperature threshold beyond which degrading thermo-oxidative reactions become discernable. Due to the semi-

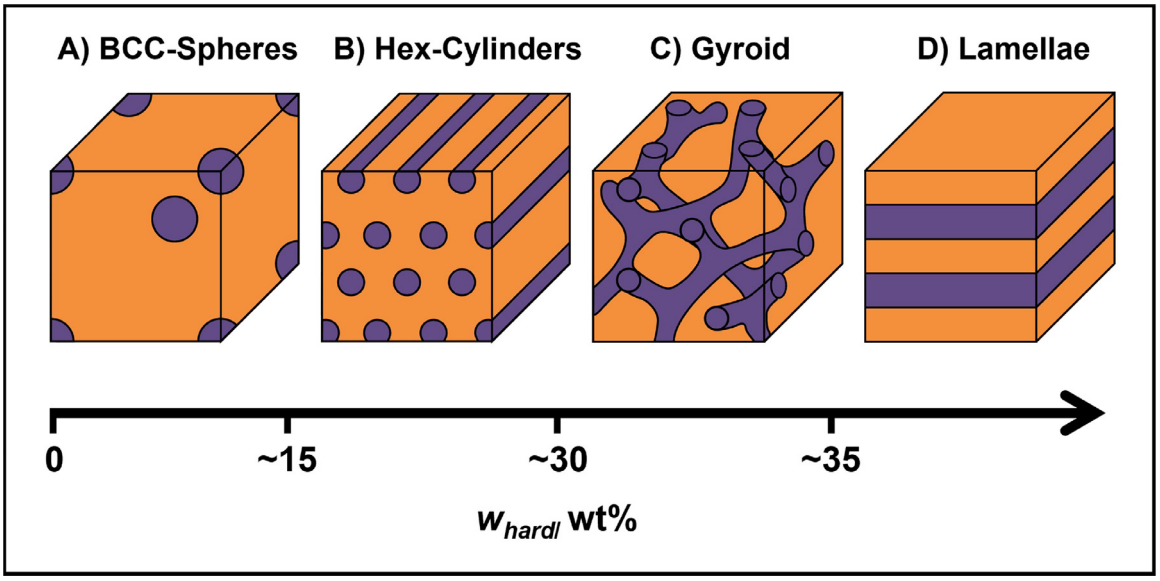

Fig. 6. A schematic showing the most common morphologies exhibited on increasing w_{hard} within a BCP composed of hard-segment and soft-segment blocks: A) BCC-Spheres: Hard-segment spheres in a Body-Centered-Cubic (BCC) structure within a continuous soft-segment domain, B) Hex-cylinders: Hard-segment cylinders arranged hexagonally in a continuous soft-segment domain, C) Gyroid: A co-continuous morphology, where both hard-segment and soft-segments exist in continuous phases, and D) Lamellae: Alternating layers of hard-segment and soft-segment domains, as w_{hard} and w_{soft} approach parity.

solid partial mixing mechanism, DSC analysis showed retention of the low-$T_{g,soft}$ and high-$T_{g,hard}$ transitions, as well as the appearance of $T_{g,mix}$ after baroplastic processing. Upon annealing at 85 °C overnight, a T_g was then seen at ≈85 °C, far above the 25 °C processing temperature, and SANS data also showed a narrowing of a previously broad peak. These observations both provide evidence of the high-T_g phase being retained and the mixed phase undergoing some amount of block de-mixing with removed pressure.

In 2003, Ryu and coworkers observed the effects of hydrostatic pressure on the closed loop behavior of a DBCP of poly(deuterated styrene)-b-poly(pentyl methacrylate) (PdS-*b*-PPMA) for this innately entropically-driven ODT [75]. SANS measurements provided confirmation for the idea of a closed loop system; χ^{eff} increased with temperature until it reached a maximum after which it began to decrease again, which is typical for systems that exhibit closed loop behavior [19,76]. It was also shown that χ^{eff} is comparable for temperatures where $T > T_{LDOT}$ and $T < T_{UODT}$; the ordered regions above a LDOT and below a UODT are identical, other than their volumes (and thus densities), which will differ due to thermal expansion. They identified the critical pressure of 6.2 MPa, at which the polymer is phase mixed at all temperatures, entirely bypassing the proposed closed loop behavior of the baroplastic. Critically, they also found that the magnitude of the LDOT and UODT transitions are similar in magnitude, however, differ in sign, thus confirming that the UODT also has a significant dependance on pressure. [27]

Soon after, in 2009, Jo et al. exploited this baroplastic behavior to demonstrate a novel data storage medium, wherein a storage density of up to 1 Tb in^{-2} could be achieved *via* nanoindentation using an Atomic Force Microscopy (AFM) tip [77]. While the exact pressure was not recorded, the extremely small (<15 nm^2) needle tip provided sufficient force (on the order of nN) to surpass 6.2 MPa and cause microphase transitions and baroplastic flow.[42] Following the generation of ultrahigh-density nanopatterns on the film by baroplastic nanoindentations, the original film could be completely regenerated in a simple heating step, enabling read/rewrite cycles. Although not the focus of this work, the exact mechanism of the ODT could not be elucidated as the change in morphology was recorded using conventional cross-sectional transmission electron microscopy (TEM) using samples from before and after the complete nanoindentation. Further investigations were conducted with *in-situ* TEM observations of the phase-transition of PS-*b*-PPMA [73]. For the first time, the transition of the BCP films from a lamellar morphology to a disordered state could be observed in real-time, helping to develop a full understanding of nanoscopic pattern formation.

Lee and coworkers carried out extensive testing on the phase-behavior of PdS-*b*-PPMA DBCP in 2006 [74]. Both SANS and Fourier transform infrared (FT-IR) spectroscopy were employed, confirming the large pressure coefficients of the closed-loop ODTs reported in previous work. The DBCP was reprocessed under medium temperature and pressure (90 °C and 5 MPa) yielding a well-defined, clear dog bone. The commercially-available Kraton G 1652 triblock copolymer (TBCP), poly(styrene)-*b*-poly(ethylene-co-butylene)-*b*-poly(styrene), of a similar MW was reprocessed similarly for comparison. The commercial material showed no baroplastic behavior, remaining a powder at 120 °C and 100 MPa. This highlighted the potential that baroplastics have to disrupt the current commercial plastics market by enabling lower temperature processing through careful choice of polymer pairs. Interestingly, the pressures used here are atypically low, at only 5 MPa, which likely explains why a temperature as high as 90 °C was required. Each baroplastic material has a pressure coefficient, which describes the change in the temperature of T_{ODT} with increasing pressure. Hence, a higher pressure would have depressed T_{ODT} by a larger amount, which may have enabled reprocessing at lower temperatures.

Work on the same DBCP, PdS-*b*-PPMA, was carried out by Kim *et al.* in 2013 [78]. Birefringence experiments demonstrated closed loop behavior through applying pressure using three different gases (argon, helium and nitrogen) as opposed to conventional hydrostatic processing. Out of the three inert gases used, only helium had the desired effect of decreasing the size of the closed-loop through increasing favorable interactions between the blocks and enhancing their miscibility similarly to hydrostatic pressure (confirmed previously by the group using SANS to determine the high pressure coefficient under hydrostatic pressure) [75]. On the other hand, pressure applied using both argon and nitrogen yielded

the opposite effect and enlarged the closed loop, promoting immiscibility of the two blocks. Critically, there was an increase in miscibility between two chemically distinct polymers when unfavorable interactions that hinder mixing were screened by the absorption of gas molecules into the DBCP [79].

In 2011, Torkelson and coworkers investigated the effects of ODTs on gradient copolymers of PS and PBA (PS-*grad*-PBA) [80]. In higher MW gradient copolymers (M_n = 95 kDa), Small-Angle X-ray Scattering (SAXS) results suggested the presence of both a LDOT and UODT. However, due to the lower segmental incompatibility of gradient polymers, when compared to BCPs with distinct blocks, high MW and temperatures were required to induce segregation of the two phases [81]. Nevertheless, the polymers were not mechanically tested, and therefore baroplastic behavior could not be confirmed with full certainty. Investigating the phase behavior of gradient copolymers as a function of pressure, both theoretically and experimentally, remains of great interest and significantly more work could be done in the area.

In 2013, Ahn et al. combined BCPs and polymer blends to investigate the phase-behavior of PS-*b*-PBA/PS-*b*-PHMA DBCP blends; a blend composed of two DBCPs which both individually undergo microphase separation [72]. PS-*b*-PBA alone shows LDOT behavior, while PS-*b*-PHMA alone shows UODT behavior. By varying the relative ratios of each DBCP in the blend, closed-loop phase diagrams could be obtained, showing an LDOT, followed by a UODT at higher temperatures. However, no calculated pressure dependance of the observed phase-behavior was reported. Further work by Ryu and colleagues investigated the pressure dependance of the same DBCP blend ODTs [82]. The DBCP blends used were analyzed using depolarized light scattering (DPLS), SANS, and DSC. While the polymer pairs demonstrated their potential to be suitable baroplastics, the polymers were not molded under pressure or tested mechanically. From SANS results, it was deduced that a peak at 0.69 MPa corresponded to ordered lamellar morphology, while at 6.2 MPa a broad peak corresponded to correlation hole scattering belonging to disordered mixing of PS-*b*-PPMA [70]. They were able to confirm the presence of an ODT through a recorded negative ΔV_{mix} at phase transitions, which is responsible for the shifting of T_{ODT} in response to pressure changes. To quantify the observed volumetric changes at transitions between ordered and disordered phases, film thicknesses were recorded in situ using spectroscopic ellipsometry under vacuum. Notably, this was conducted with varying temperature, not pressure [82], although the pressure coefficients estimated using the Clausius-Clapeyron equation were in agreement with results previously obtained from hydrostatic pressure experiments [72].

As baroplastic testing of many potential conventional acrylic, methacrylic, and styrenic monomer combinations remain unreported, a lot of fundamental research remains unexplored. A substantial amount of future work could yet be undertaken into understanding the mechanisms of new monomer combinations, which would serve to broaden the potential for replacing commodity thermoplastics with baroplastics. Furthermore, the extent of the effects of MW, molecular architectures, and morphologies within BCP baroplastics should be explored in much greater detail. Most of the BCPs discussed above focused on developing the fundamental understanding of baroplastic behavior and identifying it through techniques including DSC, AFM, TEM, SAXS, and SANS. As such, there was not a great deal of importance granted to the processability and mechanical properties of the synthesized BCPs, which are critical to any potential applications. However, there were also examples of entirely novel applications, such as high-density data storage on a baroplastic medium, which highlight the potential that baroplastics have to revolutionize many challenging areas, if correctly implemented. Importantly, there has been no probing into BCPs with greater than 2 distinct blocks, such as tri- or multi-block BCPs, which could play a substantial role in their mechanical properties.

3.3. Core-shell nanoparticles (CSNPs)

CSNPs are a class of polymer nanoparticle composed of chemically distinct and immiscible core and shell domains, which typically are not covalently linked. Instead, their morphology is maintained by phase separation of the two polymers, acting essentially as a spatially trapped polymer blend, so long as the shell exists in a rigid state. CSNPs possess properties inherent to two different materials, and have found numerous applications, such as within coatings, bio catalysis and drug delivery. Unlike BCPs, which require covalent linkages between the two phases, CSNPs can be synthesized via 2-step emulsion, dispersion, and suspension polymerization. Similarly to polymer blends and BCPs, varying the content of each polymer can affect the particle properties; however, the morphology does not inherently change, with only the respective radii of the core and shell affected (Fig. 7). In baroplastic CSNPs, the shell and core tend are composed of the high-T_g and low-T_g blocks, respectively. As can be seen in Fig. 7, due to the cubic relationship between the radius and the volume of a sphere, a CSNP with a diameter of 100 nm and a w_{hard} of 50 % would only have a shell thickness of ≈10 nm; this illustrates the importance of the hard/soft ratio, as a reasonably large w_{hard} is required simply to effectively cover the soft core. Table 2 gives the CSNPs which have been reported to show baroplastic behavior. Due to their position as a class of highly functional materials with easily modifiable properties, CSNPs are at the materials chemistry frontier of numerous electronic, biomedical, pharmaceutical and catalysis applications [83]. One key disadvantage of CSNPs is that, if full-mixing occurs due to temperatures exceeding $T_{g,hard}$, the core-shell morphology may be completely lost, yielding a less-regular and likely macroscopically phase-separated polymer blend. For comparison, this full mixing would be completely reversible with a microphase-separated BCP.

In their 2003 work [14], alongside their demonstration of baroplastic BCPs, Gonzalez-Leon et al. reported baroplastic CSNPs with PBA and PEHA soft-cores and PS hard-shells; in both cases the core was composed of a non-crosslinked low T_g polymer. Arrangement of the polymers into CSNPs allows for the two chemically distinct domains to be in close contact with one another at the nanometer scale while maintaining a controlled, well-defined structure. High MW and dispersity values are characteristic of emulsion polymerization; the high MW increases the phase separation boundary of the two components of the CSNPs. However, due to decreased polymer mobility at higher MW, slower polymer kinetics were both expected and observed. The CSNP polymers were processed at 25 °C, as shown in Fig. 5**C.i**, and could be reprocessed 10 times without showing signs of degradation to the polymer chains.

Although the above work demonstrated that PS/PBA and PS/PEHA can be reprocessed many times without significant degradation, it lacked a deeper understanding of how this pressure-induced miscibility occurred and how it could affect the resulting mechanical properties of a material; specifically when considering the effects of particle size and composition. In 2005, Gonzalez-Leon et al. investigated the same polymer pairs with a wider range of polymer weight fractions, TEM measurements, and rheology, in addition to the SANS, DSC, and tensile testing of the earlier work [84]. As may seem intuitive, the PS content within the CSNPs affected the resulting mechanical properties of the processed polymers. When w_{hard} > 50 wt%, powdery products were obtained upon precipitation from an emulsion, suggesting complete coverage of the soft PEHA cores. Similarly to previously mentioned papers, $T_{g,soft}$ and $T_{g,hard}$ were visible in DSC analysis of the dried CSNPs, as was a third T_g, attributed to $T_{g,mix}$. Measurements of the

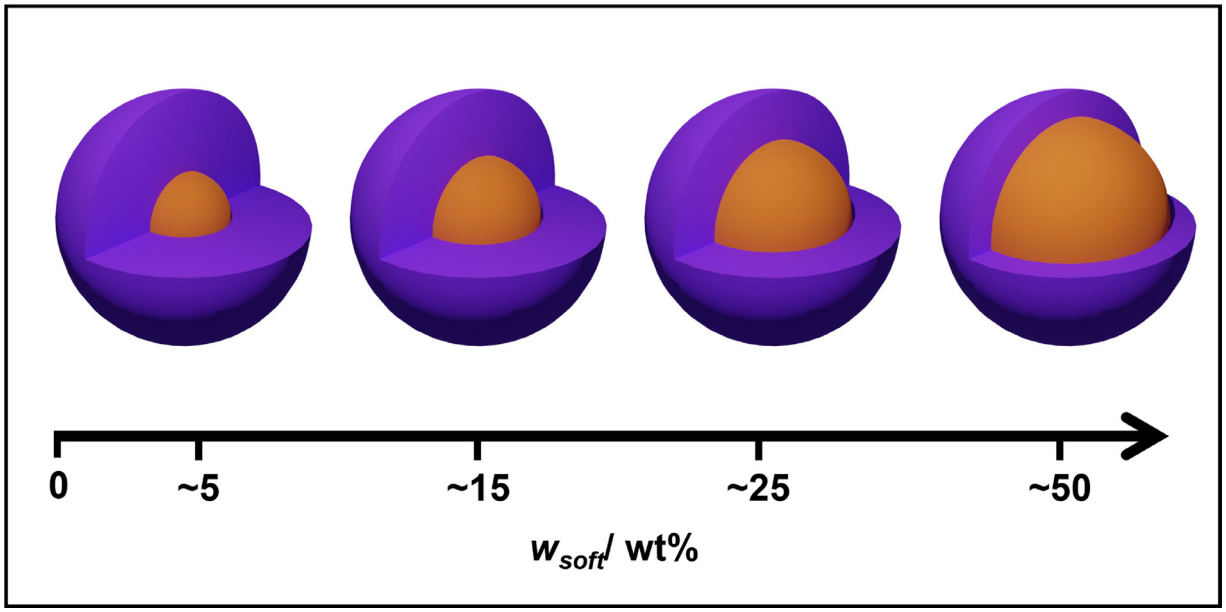

Fig. 7. A schematic depicting the effect of increasing the wt% of the soft-segment core (w_{soft}) on the shell thickness of a Core-Shell Nanoparticle (CSNP). Due to the relationship between the radius and the volume of a sphere, a high wt% of the hard-segment shell (w_{hard}) can be required to achieve effective coverage of the soft core.

Table 2
A summary of reported baroplastic CSNPs, described as Hard Shell/ Soft Core, and their nanocomposites. All were prepared through emulsion polymerization (EP).

Composition	*Polymer*					Processing			Ref.
Hard Shell/Soft Core (/inc.[a])	$T_{g,hard}$ [b] / °C	$T_{g,soft}$ [b] / °C	w_{hard} / wt%	M_n / kDa	$Đ$	Temp. / °C	Pressure / MPa	Time / min	
PS/PEHA	100	−52	66	495/303	2.22/3.00	25	34.5	5	[14,84]
PS/PBA	100	−53	63	156/112	3.08/2.29	25	34.5	5	[14,84]
PBA/PMMA	105	−53	50	n.r.	n.r.	25	35	5	[31]
PS/PBA/Silica	100	−53	73	n.r.	n.r.	25	34.5	5	[27]
PS/PBA/CNT	100	−53	50	n.r.	n.r.	25	300	10	[29]
PS/PBA/(PAA/PEO)	100	−53	50	60	2.95	25	10	10	[25]
PS/PBA/Agar	100	−53	50	70	3.0	40	10	10	[26]
PS/PBA/h-BN	100	−53	50	109/139	n.r.	25	15	10	[30]
PMMA/PBA/GO	105	−53	50	n.r.	n.r.	25	35	5	[31]
PMMA/PBA/RGO	105	−53	50	n.r.	n.r.	25	35	5	[31]

[a] (/inc) is the inclusion of a third component in a nanocomposite.
[b] Literature T_g values.

changes in specific heat capacity of the two components enabled the amount of each component within the interphase to be quantified [85–87]. The interphases were determined to be 3–5 nm thick and composed of 70–90 % PS, with ≈50 % of the total PS content involved in the mixing. These calculated interphase composition values were in good agreement with those estimated from $T_{g,mix}$ using the Fox equation. When w_{hard} < 50 wt%, obtained samples were not as powdery, which was taken as evidence of incomplete coverage of the low- T_g soft cores [87,88]. An observed shift of the SANS scattering peak to lower wavevectors after processing for periods longer than 1 min was attributed to deformation of the domains, giving larger domains in the direction perpendicular to the applied force [84]. DSC analysis corroborates this explanation, with the magnitude of the $T_{g,mix}$ transition increasing with processing time, from 1 min to 30 min, suggesting that a mixed phase was being generated over time, while under high pressure.

At 25 °C, the processing of high PS content (w_{hard} =~45–65 wt%) CSNPS produced well defined objects, whereas lower PS content CSNPs yielded a material with significant shrinkage due a more elastic nature [84]. To combat this shrinkage, the polymers were heated to 40–50 °C during the application of pressure. Regardless of the percentage of styrene content, improved processing was observed within the moderately-elevated temperature range due to increased mobility of the two phases at their interphase. A custom-made “extrusion piston” enabled the baroplastic CSNPs to be extruded, with the viscosities determined at various shear rates. The CSNPs underwent shear thinning, with the apparent viscosity decreasing from 6 to 1 MPa·s as shear rate increased from 1 to 7 s^{-1} [84], which is in the higher range of conventional polymer processing [89]. Interestingly, repeated processing had no effect on the MW of the weight-average molecular weight (M_w) = 1100 kDa PS shells, while the M_w value of the PEHA core was shown to decrease from 1280 to 595 kDa after 20 processing cycles. This was attributed to shear scission of large chains (> 1000 kDa), as a CSNP with a M_w <200 kDa PBA core showed no MW change after the same treatment [90–93]. As the mobile phase was composed of the soft core, which was released and acted as a binder between the CSNPs, only the low-T_g component underwent the shear force, explaining the unchanged MW of the PS shell [84].

The mechanical properties of the processed samples were highly sensitive to the compositional ratio, with the Young’s moduli and strain-at-break changing from 209 MPa and 400 %, respectively, at w_{hard} = 58 wt%, to 13 MPa and 1200 %, respectively, at w_{hard} = 41 wt% [84]. In terms of recovery capability after deformation, the CSNPs performed similarly to a commercial DBCP elastomer and significantly outperformed a commercial TBCP. For both lower and higher PS content CSNPs, increasing the particle size reduced Young’s modulus values and decreased the strain-at-break.

With smaller particles, the materials showed higher rigidity followed by a yielding peak in a stress-strain graph, while the larger particles gave a shallower, less rigid peak, and a shorter or absent yielding peak. As the domain sizes increased, the interfacial surface area decreased, such that the released soft component was less effective as a toughener.

Furthermore, with the overall particle diameter kept constant, the effect of decreasing the soft-core polymer MW (PBA or PEHA) was studied [84]. Decreasing the PBA or PEHA MW gave a lower strain-at-break and stress-at-break, while the Young's modulus and yield strength values showed no significant change, even when the PS shell MW also decreased. The rigidity and yield strength, then, depended specifically on w_{hard}, rather than the MW of either component, while the strain-at-break and ultimate strength were heavily dependent on the MW of the soft-core, which acted as a binder. A PS/PLMA CSNP was synthesized as a non-baroplastic reference [84], due to well-reported reduced miscibility shown by the polymers under applied pressure [22]. While the material could be processed under high pressure, the products were very weak due to a poor interphase between the CSNPs, due to the lack of released soft-core material to act as a binder [84]. These findings were reinforced by theoretical calculations conducted by the group: PS/PLMA has a positive CRS third term, representing a positive ΔV_{mix}. As such, increasing the applied pressure reduced the miscibility of the PS and PLMA domains, favoring the denser phase-separated arrangement, and explaining the lack of baroplastic flow observed for PS/PLMA.

In further work, Simonutti *et al.* successfully synthesized PS-PBA CSNPs, detecting their baroplastic potential on the single-particle scale with precise biphasic morphology [94]. Using ^{1}H NMR and ^{13}C magic angle spinning (MAS) NMR, it was confirmed that the mobility of the two phases was preserved at the nanoscale. Through the use of AFM, the CSNPs were demonstrated to possess force-responsive properties, and thus had potential to be used as sealing nano-additives in an extrinsic self-healing material.

Similarly to the BCP section above, most papers cited within this section focus on the developing the understanding of baroplastic CSNPs. While several other authors have utilized similar CSNPs (PS-PBA and PMMA-PBA) for the production of nanocomposites, as is discussed in the next section, these relied largely on existing knowledge of baroplastic CSNPs.

4. Advanced baroplastics

In much the same way as conventional thermoplastics, baroplastics can be enhanced via either careful polymer design or the incorporation of functional fillers. These advanced baroplastics can be used to enhance mechanical properties, provide additional physical properties, or incorporate bioactive components. Additionally, reducing the fraction of polymer within a given baroplastic material by combination with a filler may have the benefit of significantly reducing the manufacturing cost. Fig. 8 highlights the diverse strategies that have been explored to functionalize baroplastics and tailor them for specific applications. These approaches include the introduction of secondary bonding systems, the design of nanocomposites with improved thermal and electrical conductivity, and the utilization of heat-sensitive compounds, with each contributing to enhanced performance and application-specific adaptability. The integration of heat-sensitive compounds, in particular, is possible due to the inherent low-temperature processability of baroplastics, allowing thermal degradation to be avoided. This capability may be especially valuable in preserving the functionality of pharmaceuticals and biomolecules, positioning baroplastics as a versatile platform for cutting-edge biomedical innovations and other advanced applications.

4.1. Secondary-Bonding in baroplastics

In considering physical properties of a plastic, the strength and flexibility of the material are critical to determine its suitability to a given application. Existing baroplastics, while promising as lightweight, moldable, and recyclable materials, are limited by their unimpressive mechanical properties. The tensile strength and Young's modulus values for each series of baroplastic materials yet reported is shown in Fig. 9. Despite the importance of strength and robustness in a baroplastic, only a relatively small number of publications have sought to improve these properties. This can be accomplished either through the incorporation of secondary bonding, as will be discussed in this section, or as a by-product of a functional filler, as discussed in Section 4.2. However, in all cases, baroplastics have struggled to exceed tensile strengths of ≈11 MPa, with most modifications serving instead to increase the rigidity, thus increasing Young's modulus.

Secondary bonding can take the form of non-covalent physical supramolecular bonding, and in particular hydrogen (H-) bonding [95,96], or the form of dynamic covalent bonding [97]. Physical H-bonding crosslinking, has been the focus of both studies seeking to enhance the strength of baroplastics, via the inclusion of components which form strong H-bonds, as shown in Fig. 8**A&B**. In 2019, Lv et al. embedded poly-acrylic acid (PAA) and poly-ethylene oxide (PEO) into PS/PBA CSNPs, such that the complimentary H-bonding between PEO and PAA would strengthen the material [25]. This was accomplished by mixing aqueous solutions of the additive polymers with the CSNP emulsion, causing a white precipitate due to the extensive H-bonding. After drying, the resultant PS/PBA/(PEO/PAA) showed tensile strength and Young's modulus increases of 73 % (5.6 MPa) and 400 % (10 MPa), respectively, relative to unmodified PS/PBA CSNPs (Fig. 10**A**) [26]. Moreover, the ability to be reprocessed at ambient temperatures was maintained, with the tensile strength of several samples increasing and the strongest sample reaching 10.5 MPa on reprocessing, 3.3 times that of the initial PS/PBA CSNP (Fig. 10**B**).

Similar incorporation of H-bonding agar by Qiao et al. increased tensile strength and Young's modulus values by 265 % (8.4 MPa) and 4702 % (350.6 MPa), respectively, although reprocessing required temperatures of 100 °C to overcome the thermally-responsive H-bonding (Fig. 10**C&D**) [26]. The H-bonding was introduced within the polymer by using agar within the PS/PBA matrix. Notably, the resulting Young's modulus values were greater than for the polymer without agar incorporation. Although up to an agar loading of 20 % agar reprocessing required temperatures of 100 °C, which is the T_g of the hard-segment (PS), raising the question of whether the polymer should be classified as a baroplastic. Nevertheless, at lower agar loading (5 %) they were reprocessable at 40 °C, comfortably within the definition of a baroplastic, albeit it with a slight deterioration in mechanical properties.

It may be the case that the high temperature used could remain within the baroplastic regime, depending on its purpose. Qiao et al. noted the thermo-responsive nature of the agar, which forms coils above 90 °C, and H-bonding helices below that; such thermo-responsive behavior has been confirmed extensively in literature [98–102]. If the high temperature is only required to break the agar bonding, and not to surpass the higher T_g of PS, the term baroplastic would remain appropriate. This presents three options unexplored in this work: firstly, reprocess the materials between 90 and 100 °C, surpassing the critical agar morphology temperature but remaining below the PS T_g; secondly, substitute the hard block polymer with a higher- T_g hard block, such that 100 °C remains comfortable below the T_g; and finally, substitute agar with a different thermo-responsive system, with a transition that occurs in the 50–80 °C range. However, the second option is limited by the known suitable hard segments, which are typically just PS or

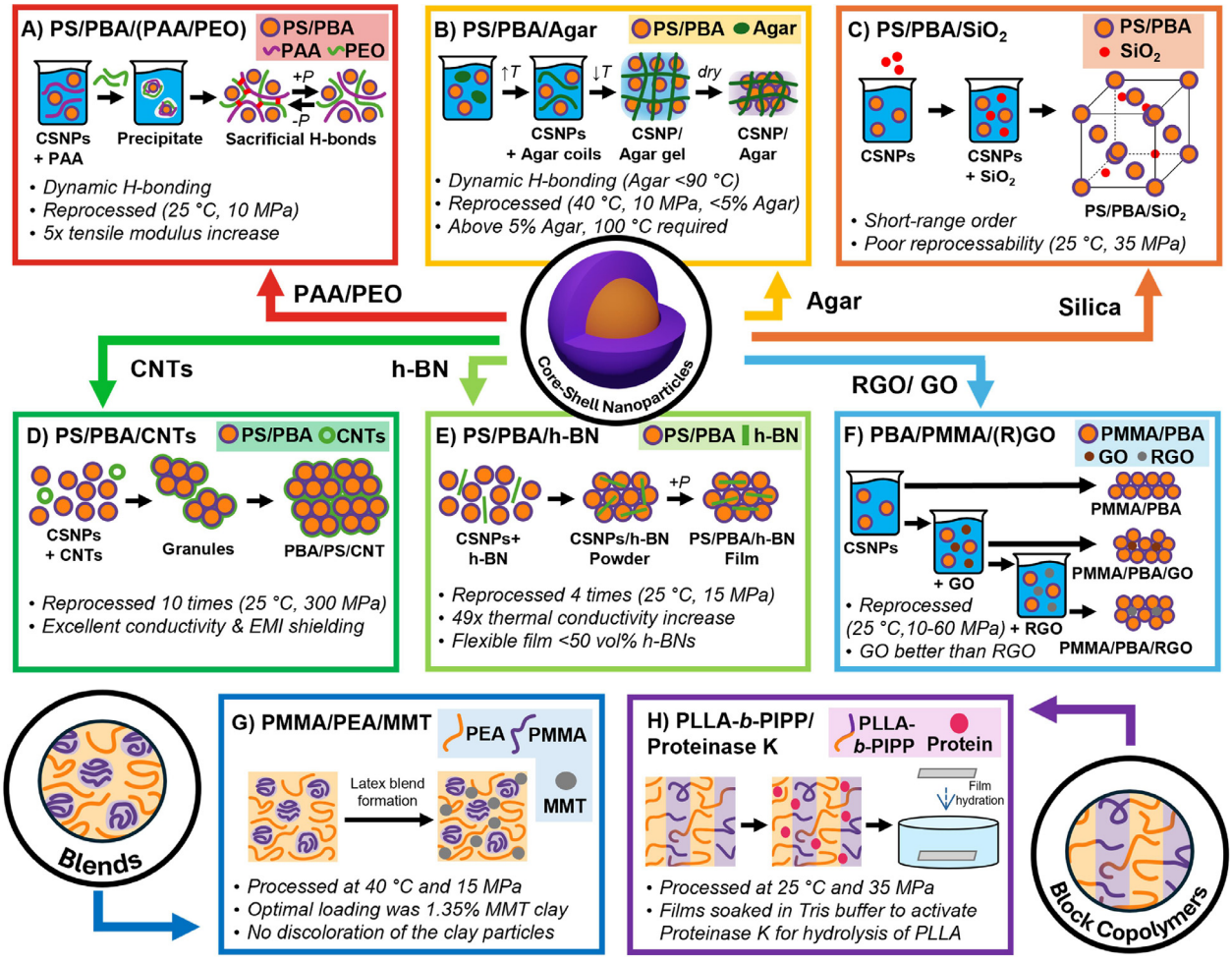

Fig. 8. A schematic overview of all reported baroplastic composites: A) PS/PBA/(PAA/PEO): PS/PBA CSNPs incorporated with poly(acrylic acid) (PAA) and poly(ethylene oxide) (PEO) for H-bonding, B) PS/PBA/Agar: PS/PBA CSNPs incorporated with agar for H-bonding, C) PS/PBA/SiO_2: PS/PBA CSNPs incorporated with SiO_2, D) PS/PBA/CNTs: PS/PBA CSNPs incorporated with carbon nanotubes (CNTs) for enhanced electrical conductivity and electromagnetic interference (EMI) shielding, E) PS/PBA/h-BN: PS/PBA CSNPs with incorporated hexagonal boron nitrides (h-BN) for enhanced thermal conductivity, F) PMMA/PBA/(R)GO: PMMA/PBA CSNPs incorporated with graphene oxide (GO) and reduced graphene oxide (RGO), G) PMMA/PEA/MMT: a PMMA/PEA polymer blend incorporated with montmorillionite clay platelets (MMT), and H) PLLA-*b*-PIPP/*Proteinase K*: a PLLA-*b*-PIPP DBCP blended with *Proteinase K* for the triggerable hydrolysis of PLLA.

PMMA, which both have similar T_g values, and the third option would have negated the novelty of utilizing agar, as described by Qiao *et al.*

Following these promising studies on simple H-bonding species, a promising research direction would be the expansion into more advanced H-bonding strategies, such as the use of host-guest complexation to create dynamic and responsive supramolecular polymer networks (SPNs) [103]. As an example of this, the ureidopyrimidinone (UPy) motif, which can form 4 H-bonds with another UPy unit, has been shown to enhance the mechanical properties of a number of polymer systems [104]. By incorporating these high-performance non-covalent interactions within baroplastics, there may be the potential to utilize these materials in soft-robotics; high-strength hydrogen bonds would provide the material with integrity [105]. The intricate mechanisms of human skin could be mimicked by incorporating biosensors, microchips, carbon nanotubes and other small electronic devices that have the ability to act provide functionality [106].

Alternatively, sacrificial covalent bonds in the form of covalent adaptable networks (CANs) could be used to attain further mechanical improvements. CANs are polymer networks with dynamic covalent crosslinks, where bonds can be made and broken in response to environmental stimuli [107]. Several CANs, responsive to a range of stimuli, have been developed in recent years as reversibly-crosslinking systems for the enhancement of material properties. These reversible chemistries include Diels-Alder (DA) (thermo-responsive) [108], thiol-disulfide exchange (light and redox-responsive) [109], boronic esters (pH-responsive) [110], and several others [97]. The incorporation of CANs into baroplastics could enable the creation of materials with robust, tunable mechanical properties and self-healing capabilities, while retaining the ability for low temperature reprocessing. Even in the case of DA, the furan-maleimide cycloaddition reaction (FMDA) is reversible above ≈100–150 °C [111], while other diene-dienophile pairs typically require temperatures in excess of 250 °C to show reversibility [112]. Temperatures above 100 °C may seem untenable in a process termed “low-temperature”, however FMDA chemistry is also reportedly mechano-responsive, such that reprocessing under high pressure may serve to cleave the reversible crosslinking, even at mild temperatures. By combining the pressure-responsive nature of baroplastics with the varied stimuli-responsive nature of CANs and SPNs, it may be possible to develop materials with unprecedented control over their mechanical, thermal, and processing properties.

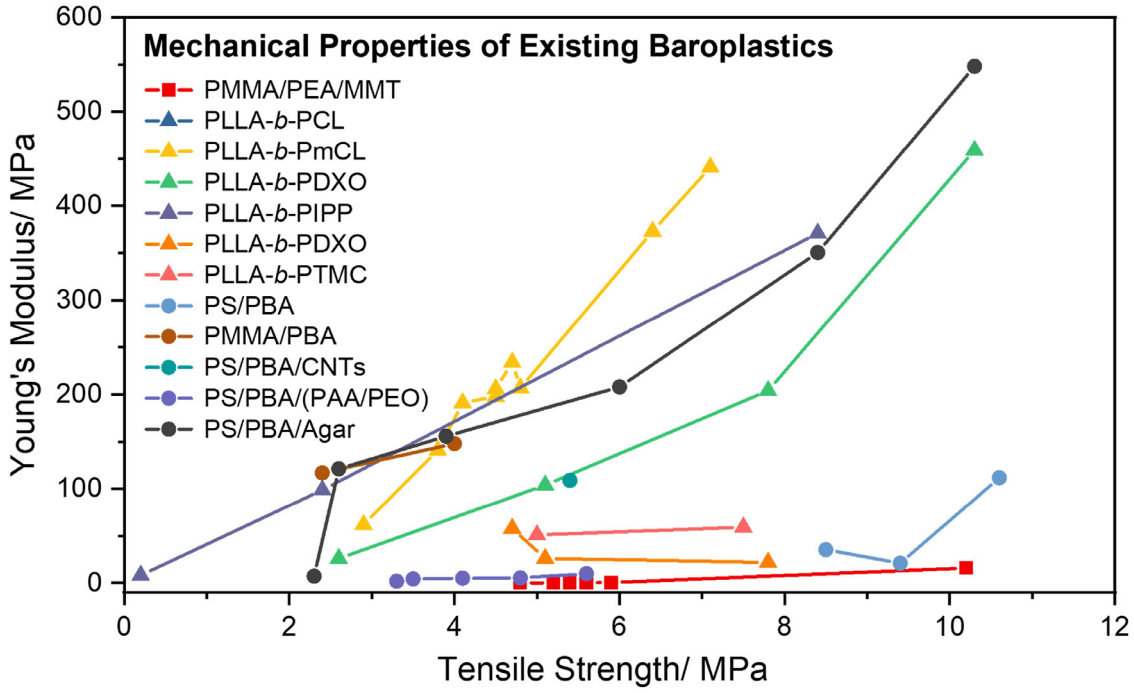

Fig. 9. All reported Young's Modulus and Tensile strength values of baroplastic materials between 2003 and 2024, with each experimental series shown as a series of data points to highlight the upper and lower recorded limits of each material. Polymer blends are shown with squares, BCPs are shown with triangles, and CSNPs are shown with circles.

4.2. Functional baroplastic nanocomposites

When looking to apply baroplastic materials to specific applications such as medical grade packaging, adhesives, and electrical conductors, the specific material properties required must be considered. Beyond simply improving mechanical properties, nanocomposites of baroplastics with functional fillers have been utilized in a number of studies, in order to provide additional material functionality. While polymer blends, BCPs, and CSNPs are all capable of modification in this way, the majority of studies have focused on PS/PBA and PMMA/PBA CSNPs due to their reliable performance. The CSNP modifications which have been used to achieve properties including electrical and thermal conductivity, are summarized in Fig. 8**C-F** [25–32].

In the earliest example of PS/PBA CSNP modification, Hewlett investigated the incorporation of silica to create a baroplastic nanocomposite (PS/PBA/SiO_2) [27]. Both pre-emulsion (creating a core-shell-shell morphology) and post-emulsion (yielding crystalline coordination between silica and CSNPs) strategies were utilized to incorporate the silica particles within the matrix. However, both methods yielded nanocomposites with poor processing properties, to the extent that mechanical testing could not be performed. This elucidated the role of interfaces and phase separation in baroplastic nanocomposites, since phase separation resulted in reduced interfacial connection and poor dispersion of inorganic material. An investigation into the crystal structure of the material identified a "zinc-blende"-type structure of the CSNPs and SiO_2 molecules with short-range ordering, but no long-range ordering. A subsequent loss of mechanical strength, relative to pure PS/PBA CSNPs, was observed, providing evidence for the conclusion that good dispersion must be attained for strong interfacial interactions, and thus strong mechanical properties.

Work by Lv *et al.* demonstrated baroplastic-carbon nanotube composites (PS/PBA/CNT) which were reprocessed at 25 °C and 300 MPa, with the purpose of improving electromagnetic interference shielding efficiency (EMI SE) by introducing high conductivity [29]. The addition of 3.0 wt% carbon nanotubes (CNTs) to the existing PS/PBA matrix via mechanical mixing, and then compression molding, of PS/PBA and CNT powders resulted in a new, highly conductive material with excellent EMI SE performance (Fig. 11**A**). Similarly to other baroplastics, the new material showed remarkably little performance drop-off with reprocessing. Although the strain-to-break decreased from 61.2 to 40.6 % between the 1st and 4th cycles, it then stabilized and remained above 33 % after 10 cycles. Similarly, the stress-at-break and Young's modulus values were very stable, changing from 5.4 MPa and 108.9 MPa, respectively, after 1 cycle, to 4.3 MPa and 114.4 MPa, respectively, after 10 cycles. While conductivity also decreased over the first 5 cycles, from 30.2 to 16.2 S m^{-1}, a value of 13.3 S m^{-1} was retained after 10 cycles, with only a 16 % decrease in conductivity over the latter 5 cycles.

EMI SE performance was measured in dB over a frequency range of 8–12 GHz, with an average value also calculated across the whole range. Between the 1st and 2nd cycles, performance loss mainly occurred at higher frequencies, after which any further decreases were consistent across the entire frequency range [29]. The average ESI SE decreased from 38.9 to 28.5 dB between the 1st and 4th cycles, before stabilizing to give 24.3 dB after the 10th cycle (Fig. 11**B**). Even after 10 cycles, the 20 dB target EMI shielding level for commercial applications was comfortably exceeded, which represents the capability to block 99 % of incident EM waves. Increasing the CNT loading from 3.0 to 5.0 wt% gave an ultra-high EMI SE of 45.1 dB, while using only 0.5 wt% CNT gave an EMI SE of 19.2 dB, almost meeting commercial requirements. Lv *et al.* discussed the preservation of conductive networks within the material on reprocessing as an explanation for the relatively stable conductivity and EMI SE. Finally, they compared the lack of heat required for reprocessing the baroplastic composite with the heat required for comparable EMI shielding materials, such as high-density polyethylene (HDPE) and polypropylene (PP), which

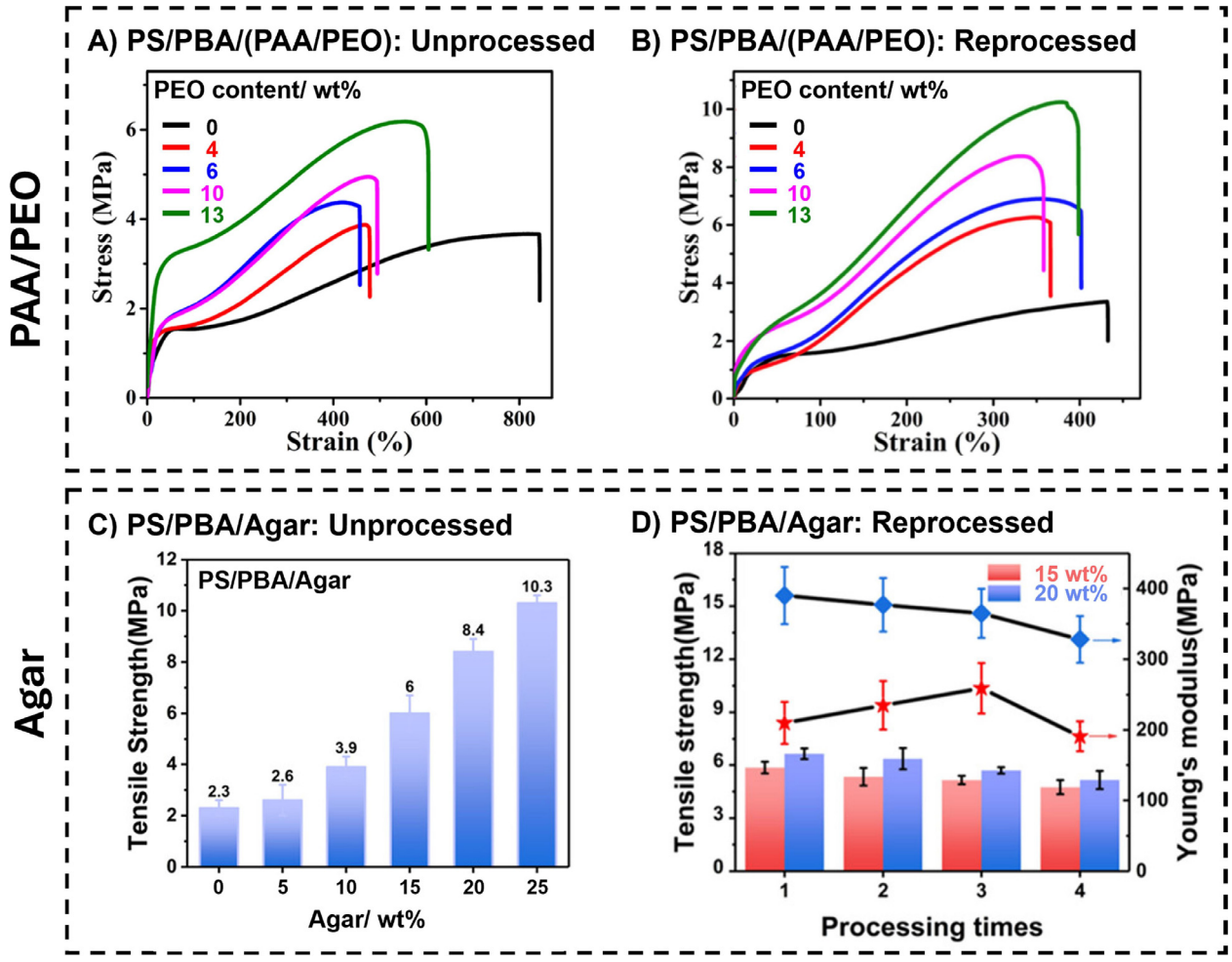

Fig. 10. The stress strain curves of PS/PBA CSNPs modified with varying equimolar amounts of poly(acrylic acid) (PAA) and poly(ethylene oxide) (PEO) as H-bonding additives A) during their initial tensile testing, and B) after reprocessing.([25]. Copyright 2019. Adapted with permission from the American Chemical Society.) C) The tensile strength of PS/PBA CSNPs modified with varying amounts of Agar as a H-bonding additive, and D) the preservation of mechanical properties after a number of processing cycles at 100 °C. ([26]. Copyright 2020. Adapted with permission from the American Chemical Society.).

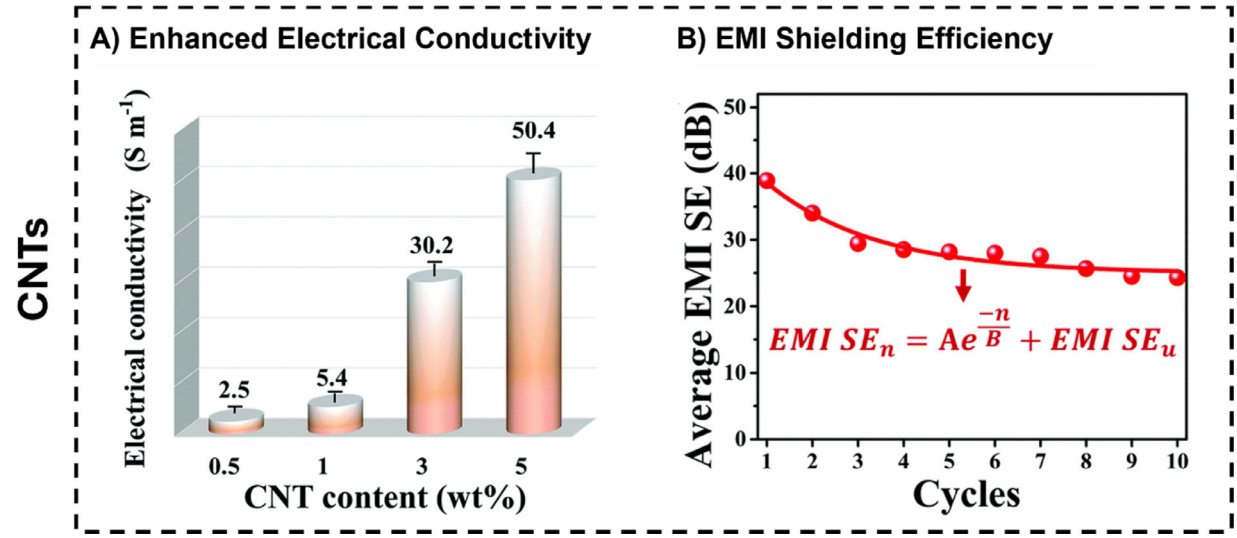

Fig. 11. A) The effect of incorporating Carbon Nanotubes (CNTs) into baroplastic PS/PBA CSNPs on their electrical conductivity, and B) The Electromagnetic Interference Shielding Efficiency (EMI SE) performance of the resultant PS/PBA/CNT baroplastic after a number of reprocessing cycles. ([29]. Copyright 2018. Adapted with permission from the Royal Society of Chemistry.).

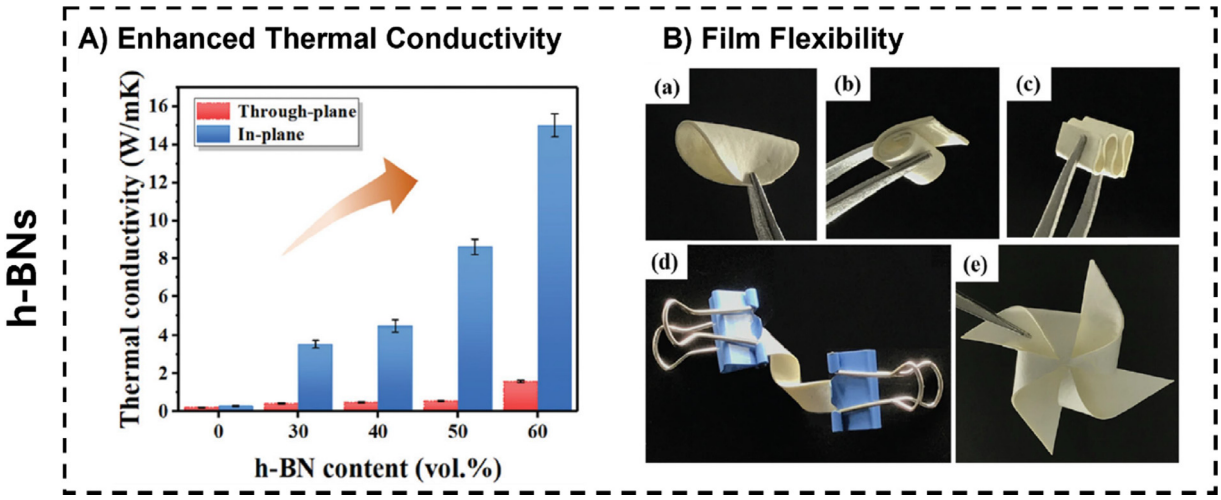

Fig. 12. The effect of incorporating hexagonal boron nitrides (h-BNs) into baroplastic PS/PBA CSNPs on their thermal conductivity, and B) The flexible and shapeable nature of resultant PS/PBA/h-BNs films. ([30]. Copyright 2021. Adapted with permission from the Royal Society of Chemistry.).

have heat processing requirements of 357 and 337 J g^{-1}, respectively, highlighting the impressive energy savings achievable with their approach [29].

Further investigation carried out by the same research group involved the incorporation of hexagonal boron nitrides (h-BNs) into the PS/PBA CSNP matrix, in order to produce PS/PBA/h-BN thermal management composites with high heat-dissipation capacities [30]. PS/PBA CSNPs were loaded with 30, 40, 50, and 60 vol% h-BNs, which increased the thermal conductivity of the virgin PS/PBA by a factor of 12, 14, 28, and 49, respectively (Fig. 12**A**). Due to alignment of the platelet-shaped h-BNs, the materials showed anisotropic thermal conductivity, with high in-plane conductivity and low through-plane conductivity. The degree of orientation increased with h-BN content from 30 to 50 vol%, attributed to uniform dispersions of h-BN within the matrix, before decreasing slightly at 60 vol%, attributed to an increase in disorder due to high h-BN content. The PS/PBA/h-BN composite with 50 vol% h-BN achieved a thermal conductivity of close to 9 W m^{-1} K^{-1}, while maintaining the flexibility to be bent, curled, and twisted into a windmill shape (Fig. 12**B**). At 60 vol% h-BN, the composite had a lower flexibility, but reached a high thermal conductivity value of 15.1 W m^{-1} K^{-1}. The Shore A hardness of the PS/PBA/h-BN composites increased from 58 to 81 HA on increasing h-BN loading from 30 to 60 vol%, comfortably within the 50 to 90 HA hardness range of a number of commercial thermal management materials [30].

The thermal conductivity of a 60 vol% h-BN sample decreased by 5 % after 1500 bending cycles, and by 15 % on being heated from 25 to 100 °C, showing remarkable stability in both cases [30]. When applied as a heat-spreader to a test ceramic heater, the temperature reached by the 60 vol% h-BN sample was 36 % lower than the temperature reached by a blank control without a heat spreader, highlighting its excellent thermal dissipation efficiency. Interestingly, these baroplastic materials could be reprocessed at 25 °C and only 15 MPa, far lower than the 300 MPa utilized in their previous work, despite utilizing similar PS/PBA matrices. The materials became brittle beyond 60 vol% h-BNs, as well as less smooth and uneven at lower h-BN content (30 and 40 %), due to imperfect balances of the PBA soft component with the rigid h-BN. Crucially, the thermal properties across the whole range of h-BN loadings were retained upon reprocessing 4 times, providing a recyclable alternative to commercial thermal management products such as thermal silicon pads.

As with BCPs, CSNPs with PMMA hard segments have also been explored. Tang et al. prepared PMMA/PBA CSNPs via emulsion polymerization, and then incorporated graphene oxide (GO) within the latexes (≈0.5 wt% GO loading) [31]. This was, in some cases, reduced further to give incorporated graphene (reduced graphene oxide, RGO). The PMMA/PBA CSNP synthesis yielded solid powdery materials upon demulsification and freeze drying. These unmodified PMMA/PBA CSNPs showed baroplastic flow during processing at 25 °C and 35 MPa to give transparent films. The PMMA/PBA/GO and PMMA/PBA/RGO composites could also be processed under the same conditions, with the former transforming from a light-brown powder to a black film, and the latter transforming from a grey powder to a black film [30].

Notably, for all reported polymers, longer processing times (from 3 to 9 min at 35 MPa) and higher applied pressures (from 15 to 55 MPa for 5 min) resulted in better mechanical properties, due to the material having more time, or less resistance, to flow, respectively (Fig. 13) [31]. However, the increase in yield strength across each series remained <1 MPa, with the highest recorded yield strength in all cases remaining below 4.1 MPa. Similarly, the Young's Modulus values varied by <30 MPa, with the highest recorded value of 148 MPa. The Young's modulus values of PMMA/PBA were increased by incorporating both GO and RGO due to their rigidity. The incorporation of GO made little difference to the tensile strength of PMMA/PBA/GO in all cases, although the incorporation of RGO significantly lowered the tensile strength of PMMA/PBA/RGO by about 1 MPa, in all cases. According to TEM, the GO-containing CSNPs showed improved dispersion and a stronger interphase with the matrix, when compared to both the pure and RGO-containing CSNPs. The increased hydrophobicity of the graphene sheets (RGO) generated from the reduction of GO resulted in re-agglomeration in the RGO-containing CSNP sample. The increased homogeneity of the GO-containing CSNPs was attributed to the oxygen groups within the GO sheets, which could form H-bonds with pendant carbonyl chains within the CSNP polymers) [31]. The significant impact that switching from GO to RGO had on the mechanical properties of these baroplastics highlights the dramatic effects that subtle material design changes can have. Disappointingly, this work reported no repeated processing cycles, such that the possibility of aggregation of GO or RGO over time was not interrogated.

The modification of baroplastic polymer blends has also been conducted. In 2006, Xu et al. improved upon the properties of a

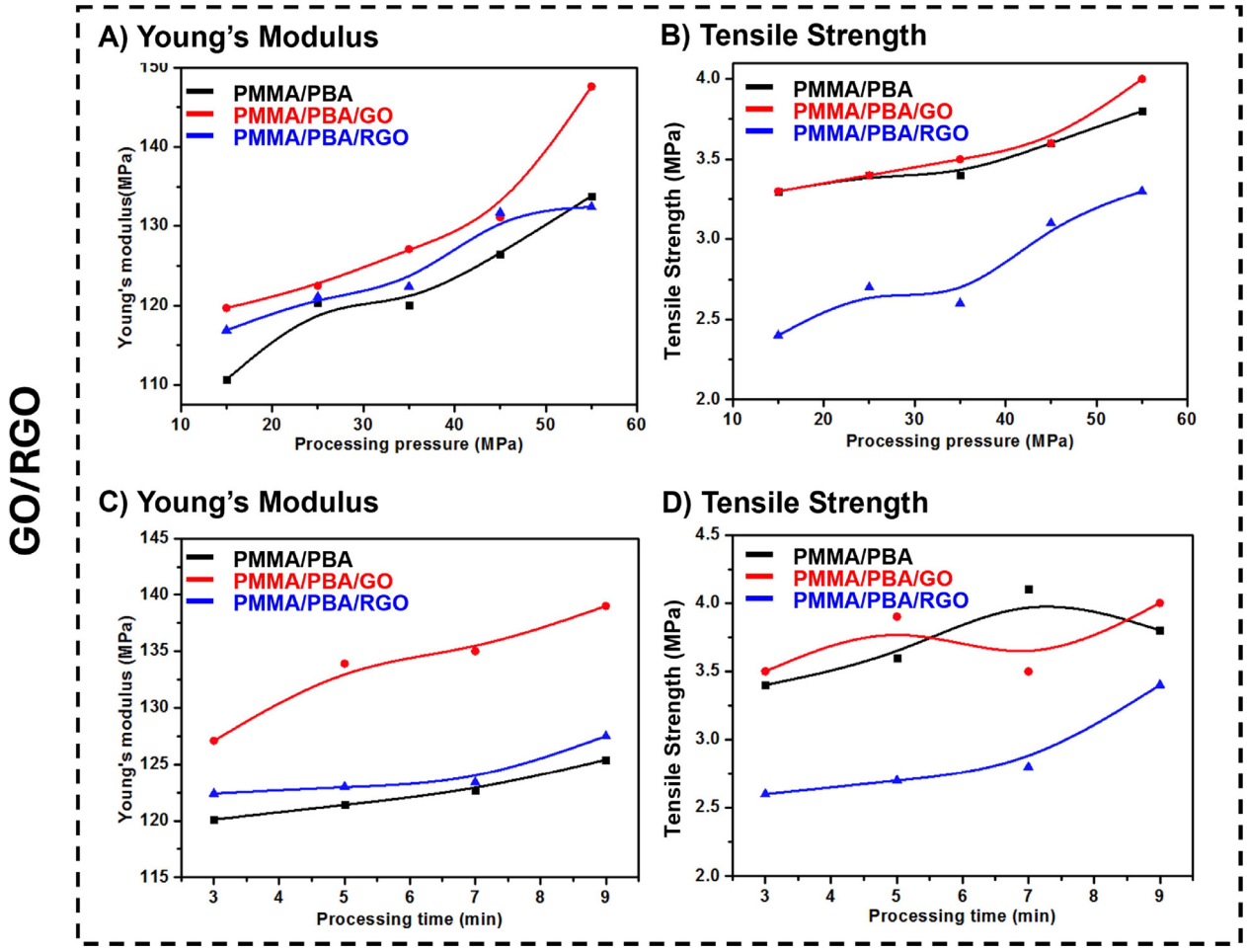

Fig. 13. The mechanical properties of PMMA/PBA CSNPs unmodified and modified with graphene oxide (PMMA/PBA/GO) and reduced graphene oxide (PMMA/PBA/RGO). A) Young's modulus and B) Yield Strength after processing for 5 min at 25 °C under varying pressures. C) Young's modulus and D) Yield Strength after processing at 25 °C and 35 MPa for varying lengths of time. ([31]. Copyright 2014. Adapted with permission from Institute of Physics Publishing Ltd.).

PMMA/PEA emulsion blend by incorporating a homogenous dispersion of 1.59 % montmorillionite (MMT) clay platelets into the existing cationic latex through heterocoagulation [32]. They demonstrated that the nanocomposites could be processed at low temperatures (40 °C, 15 MPa), without the discoloration that typically occurs when processing thermoplastic nanocomposites due to thermo-oxidative reactions [66]. Improved tensile strength (+23 %) and Young's modulus (+120 %) confirmed the reinforcing effect of the MMT within the blend, even with a low loading of 1.59 % [32].

The advancements in baroplastic materials through their combination with a range of functional components underscore their versatility and potential for use within high-performance applications. The ability to implement and tune functionality through the design of nanocomposites has opened doors to enhanced mechanical strength, thermal stability, and electrical and thermal conductivity, while preserving low-temperature reprocessability. Despite challenges such as achieving uniform dispersion and interfacial compatibility, studies on materials like PS/PBA with silica or CNTs, and PMMA/PBA with GO, have demonstrated significant progress in overcoming these barriers, with very promising results. These findings highlight the importance of optimizing composition and processing conditions to unlock the full potential of baroplastic composites. As research continues to refine these materials and broaden the range of incorporated materials, their potential applications across diverse fields—from medical packaging to thermal management—will undoubtedly expand.

4.3. Bioactive baroplastics

One of the main advantages unique to the baroplastic processing mechanism is their ability to be recycled at low and ambient temperatures. Existing thermoplastics are mostly processed via melt-molding at high temperatures (>180 °C) which can be extremely damaging to any incorporated biomolecules, which are typically deactivated or destroyed. The ability of baroplastics to be processed at mild temperatures, without thermal material degradation, open up a series of possible uses including biomedical, therapeutic, and drug-delivery applications, *via* the incorporation of useful heat-sensitive materials into polymeric matrices.

Notably, there have only been two studies in this research area despite its evident potential; a large amount more fundamental work needs to be undertaken to effectively harness such possibilities. In the 2016 study by Taniguchi and coworkers, novel polyester-based BCP baroplastics were identified and then implemented as a matrix for biomolecules, demonstrating the first reported bio-functional baroplastic composite capable of catalyzing its own hydrolysis [28]. Specifically, this work involved the inclusion of *Proteinase K*, a fungal enzyme capable of catalyzing the degradation of poly(lactide) (PLA) [113], within a DBCP of poly(L-lactide) and poly(2-Isopropoxy-2-oxo-1,3,2-dioxaphospholane) (PIPP). The DBCPs were synthesized by ring opening polymerization of L-lactide with a PIPP macroinitiator and could be processed at 35 °C and 35 MPa. SAXS at ambient pressure revealed a strong peak attributed to the periodic struc-

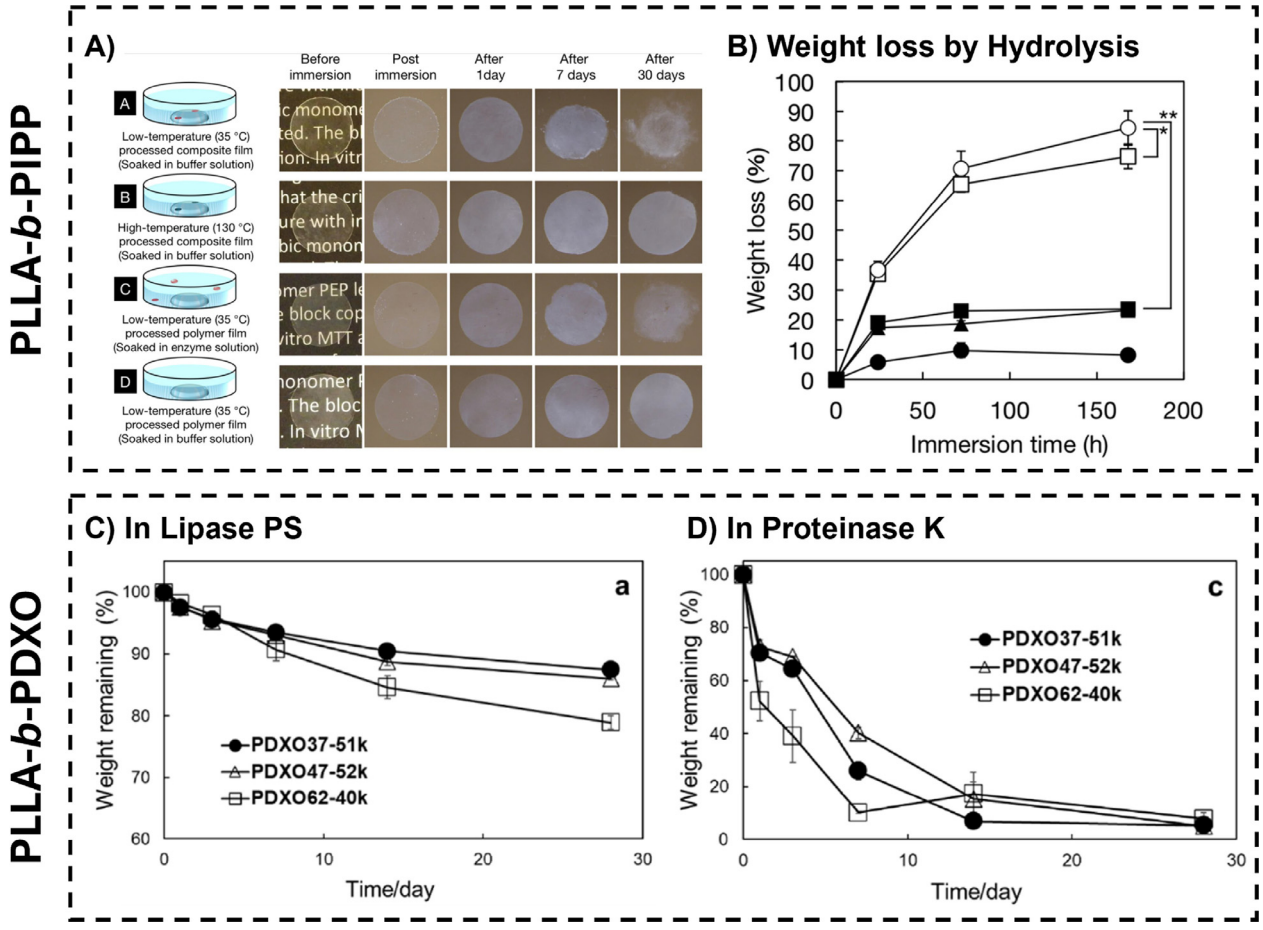

Fig. 14. A) A study of the biodegradability of PLLA-*b*-PIPP DBCPs with incorporated *Proteinase K* by soaking in a buffer solution after processing at low and high temperatures, and B) the weight loss monitored over 7 days, with the hollow shapes representing the low-temperature processed sample and the positive control, and the solid shapes representing the high-temperature processed sample and the negative control. ([28]. Copyright 2016. Adapted with permission from the American Chemical Society.) C) The biodegradation of a PLLA-*b*-PDXO DBCP over 4 weeks in a *Lipase PS* solution, and D) The same biodegradation in a *Proteinase K* solution. ([113]. Copyright 2024. Adapted with permission from Elsevier Science Ltd.).

ture of the microphase separation between PIPP and PLLA, with an average structural length of 14.8 nm. This peak was greatly diminished after the application of 50 MPa of pressure, but returned to its original height under the removal of the pressure, providing strong evidence that the increased pressure is causing temporary miscibility between otherwise immiscible domains. The amount of crystallinity within the DBCPs was quantified by both DSC and X-Ray Diffraction (XRDs), which both showed increasing crystallinity with increasing PLLA block length. Increasing the PLLA content from w_{hard} = 46 wt% to w_{hard} = 61 wt% increased the tensile strength and Young's modulus values from 0.2 MPa and 8.3 MPa, respectively, to 8.4 MPa and 371 MPa, respectively. Clearly, the PLLA fraction within the DBCPS had a massive impact on their mechanical properties, which largely dictates the applications for which they may be suitable. Although the effect of reprocessing on mechanical properties was not investigated, XRD patterns were identical after 4 reprocessing cycles, suggesting that a similar amount of crystallinity was retained on reprocessing [28].

Bio-composites were prepared by mixing the DBCPs with proteinase K in the solid phase and compression molding at 35 °C and 35 MPa for 5 min [28]. Disc-shaped films were soaked in Tris buffer solution (pH 9.0) in order to activate the *Proteinase K*, causing them to swell due to the hydrophilicity of the PIPP. As shown in Fig. 14**A&B**, the hydrolysis of the PLLA blocks occurred mostly within 7 days, while a control sample processed at 130 °C remained unchanged after 30 days due to the high temperature denaturing the enzyme. Crucially, the function of the *Proteinase K* was preserved via low-temperature processing, highlighting the potential for incorporating thermally-sensitive components into baroplastics for a whole range of biomedical materials [28,114].

Very recently, in 2024, the same research group studied the degradation of PLLA-*b*-PDXO DBCPs with *Lipase PS*, an esterase which is selective for non-PLA aliphatic polyesters, and *Proteinase K* [113]. Notably, the baroplastic behavior of the BCPs was not harnessed for the incorporation of enzymes, with the degradation simply studied by immersing polymer samples into solutions of *Lipase PS* and *Proteinase K*. The degradation of the PLLA-*b*-PDXO polymers in *Lipase PS* was highly dependent on the soft-segment PDXO content. 20 % weight loss after 4 weeks was observed when w_{soft} = 62 wt%, while a w_{soft} value of $\leq$ 47 % showed no significant degradation over the same time, attributed to the relative hydrophobicity of PLLA (Fig. 14**C**). Contrastingly, *Proteinase K* was very effective in the degradation of the PLLA-*b*-PDXO polymers, achieving over 90 % weight loss after 4 weeks in all cases, highlighting the importance of enzyme selection (Fig. 14**D**). While the MW of the DBCPs did not have a significant direct effect on degradability, reducing the size of the PLLA blocks reduced the crystallinity of the semicrystalline PLLA, which slightly enhanced the rate of degradation as amorphous regions could better fit into the *Proteinase K* binding sites [113].

Although the incorporation of biomolecules within baroplastics is still in its early stages, these proof of concepts signifies

its promise as a research avenue. The ability to process these materials under mild conditions, avoiding the thermal degradation common with traditional biodegradable polymers, paves the way for innovative applications such as drug delivery systems, bio-functional films, and advanced biomedical materials. Despite the progress, the limited exploration of this field leaves a significant opportunity for further research to fully realize the potential of combining baroplastics with biomaterials, with only one paper actually demonstrating the preservation of a biomaterial through low-temperature processing.

5. Sustainable baroplastics

To be able to make an informed judgment on both the long- and short-term impact of baroplastics, a thorough evaluation of their environmental footprint is essential. This includes assessing their potential alignment with current trends in sustainable plastic innovation, such as the use of renewable or bio-based feedstocks for monomer synthesis, energy-efficient reprocessing techniques, and recycling methods that support a shift toward a circular economy. By integrating these principles, baroplastics could contribute to reducing waste and dependence on fossil-based resources, ultimately positioning themselves as a viable, sustainable alternative within the evolving materials landscape.

As of 2023, over 90 % of global plastic production still utilized finite petrochemical feedstocks [115]. Renewable resources, primarily biomass and CO_2, provide routes to produce historically petrochemically-sourced monomers, as we recently reviewed in detail [116], and opens up opportunities to produce a wide range of new polymer structures [117]. Bio-degradable polymers, often considered a solution to plastic pollution due to their ability to fully degrade in the environment, are sometimes incorrectly conflated with bio-based polymers. However, this is likely due, in part, to the significant overlap of the types of polymers in each classification, in particular aliphatic polyesters [118]. Nevertheless, a number of polyester-type polymers, such as PLA, polyhydroxyalkanoates (PHAs) and polybutylene succinate (PBS), can be both obtained from sustainable feedstocks and degraded in the environment or via industrial composting, presenting an attractive option for developing “greener” plastic solutions [119]. It might be imagined that the production of bio-based and bio-degradable plastics is at odds with the end-goal of baroplastics, which is to facilitate a closed-loop plastics economy. However, this is not the case. Even the most polished closed-loop recycling system would inevitably lose some material to the environment, in which case degradation of such litter would be ideal. Similarly, some polymer production will always be required, either to compensate for inevitable losses or due to growing demand, in which case utilizing sustainable feedstocks is greatly preferential to consuming finite petrochemical sources.

As the baroplastic field is still relatively young, it is the perfect time to try and incorporate environmentally-friendly properties directly into polymers. This intuitive approach stands in sharp contrast with the current global ordeal of attempting to retrofit “green” plastics into a well-established plastics economy. One critical issue encountered with aliphatic polyester recycling is their especially severe degradation during melt-processing [120,121]. As a result, aliphatic polyesters are scarcely recycled via thermal methods and so typically accumulate in landfills and the wider environment. When recycled under pressure using a baroplastic mechanism, aliphatic polyesters become demonstrably more attractive due to their extended lifetime and enhanced recyclability, relative to thermally-reprocessed polyesters [15,16,28,122]. As opposed to conventional polymers derived from petrochemicals, aliphatic polyesters have the added benefit of often being bio-based (Fig. 15) [123]. Broadening the use-cases of such polymers would, as a result, provide a more sustainable route to various packaging materials, biomaterials (such as wound dressings and sutures), and biopolymers used in agricultural applications, among others [124]. Thus far, the only polyester-type polymer exploited as a hard-segment for baroplastic materials is PLLA, while there have been several tested soft-segments; the range of polyester structures prepared in recent years leaves this research area ripe for the identification and utilization of further baroplastic polyester pairs.

In 2012, Taniguchi and Lovell synthesized a series of biodegradable aliphatic polyester BCPs with 2-step ring-opening polymerization (ROP), which displayed baroplastic behavior under 34.5 MPa of hydraulic pressure at ambient temperatures [16]. The DBCPs were composed of high-T_g PLLA and low-T_g PCL, its derivative poly (caprolactone-*r*-5-ethylene ketal caprolactone) (PmCL), or poly-1,5-dioxepan-2-one (PDXO) (Table 3). Unlike previous BCPs, the high-T_g component, PLLA, was relatively low at around 60 °C, but importantly PLLA is crystalline with a melting point around 150 °C. Notably, only PLLA was derived from renewable feedstocks, with the remaining polymers were synthesized from petrochemical sources, although a number of routes to PCL from biomass exist [125]. When the PLLA content was between 40 and 60 %, PLLA-*b*-PmCL and PLLA-*b*-PDXO DBCPs could be processed at 25 °C and 34.5 MPa for 5 min to give transparent objects [16]. However, the PLLA-*b*-PCL DBCP required a temperature of 65 °C to be processed, due to the semi-crystalline nature of PCL, which has a melting point at 58 °C. Notably, this temperature also likely surpassed the ≈60 °C T_g of the PLLA hard-block, such that any PLLA chains within amorphous regions may have gained extra mobility, even without a baroplastic mechanism. While the obtained products were initially transparent, they became opaque within a week at 25 °C, or a day at 80 °C, due to the crystallization of PCL. Both extrudates and clear, thin films were obtained from the original solid powder, and as further evidence of the baroplastic mechanism, a decrease in lamellae structure with increasing hydraulic pressure was observed using SAXS, confirming the presence of an ODT during processing.

The mechanical properties of both PLLA-*b*-PmCL and PLLA-*b*-PDXO DBCPs followed similar trends, with tensile strength increase with PLLA content [16]. On increasing the PLLA content from 47 to 57 %, the tensile strength of PLLA-*b*-PmCL DBCPs increased from 2.9 to 6.4 MPa, and on increasing the PLLA content from 40 to 61 %, the tensile strength of PLLA-*b*-PDXO DBCPs increased from 2.6 to 10.3 MPa. The mechanical properties of the PLLA-*b*-PCL DBCP, however, was far superior, achieving a tensile strength and Young’s modulus of 38 MPa and 950 MPa, respectively, which was likely due to the semi-crystalline nature of both of the polymer blocks. Other than the PLLA-*b*-PCL DBCP reported in this work, which arguably shouldn’t qualify as a baroplastic, the PLLA-*b*-PDXO DBCP with 61 % PLLA appears to be the strongest baroplastic BCP reported thus far, achieving a tensile strength of >10 MPa despite containing an amorphous soft-block.

When a PLLA-*b*-PmCL sample was processed conventionally at 200 °C for 30 min, GPC analysis showed the M_w to decrease from 158 to 121 kDa and the $Đ$ to have increased from 1.8 to 2.0, showing clear signs of thermal degradation of polymeric chains [16]. When processed at 25 °C, the GPC traces before and after processing were identical, with no increase to PDI and no low-MW fractions formed, providing excellent evidence that polymer degradation was fully avoided during low-temperature compression processing. Notably, the crystallinity of the blocks within the BCPs plays a critical role in the baroplastic mechanism of the material. Crystallinity is not considered within the aforementioned CRS model, which becomes an issue when working with biodegradable comonomers in the form of polyesters, as they are often semi- or fully crystalline [16,28]. An additional obstacle to overcome may be

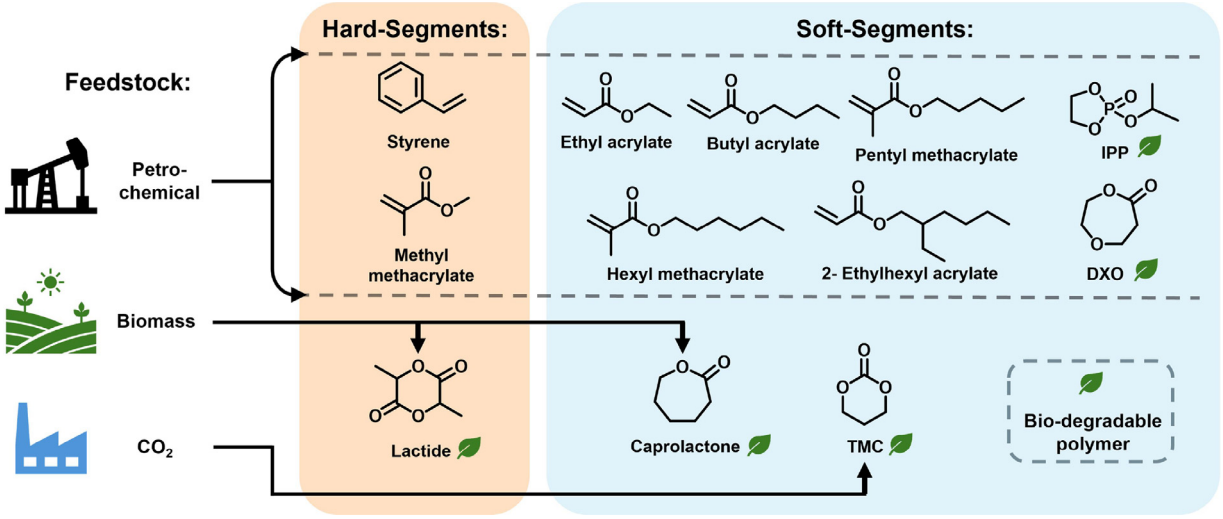

Fig. 15. The monomers utilized in low-temperature baroplastics, with their feedstocks and potential for bio-degradability shown.

Table 3
A summary of reported polyester and polycarbonate-based baroplastics, prepared via ring opening polymerization (ROP), and described as (hard-*b*-soft).

Composition	*Polymer*					Processing			Ref
(hard-*b*-soft)	$T_{g,hard}$ [a] / °C	$T_{g,soft}$ [a] / °C	w_{hard} / wt%	M_n / kDa	$Đ$	Temp. / °C	Pressure / MPa	Time / min	
PLLA-*b*-PmCL	60–65	−58	48	66	1.5	25	34.5	5	[16]
PLLA-*b*-PDXO	60–65	−32	53	184	1.5	25	34.5	5	[16,113]
PLLA-*b*-PCL	60–65	−60	44	203	1.3	25	34.5	5	[16]
PLLA-*b*-PIPP	65	−41.5	53,4	n.r.	1.5	25	35	5	[28]
PLLA-*b*-PTMC	50	−17	65	34	n.r.	36	50	5	[15]

[a] Literature T_g values.

the interference of the crystallinity on the pressure induced mechanism, although this has yet to be proven, presenting an obvious and important concept to be explored. Nevertheless, the benefits of a having a crystalline block, such as strength and resistance to hydrolysis, may make them desirable candidates for the development of novel baroplastic materials with relevant applications. It is also possible that altering the tacticity of the polymer or introducing side-chains to the monomers could increase the amorphous character, and thus mobility, of the polymers, encouraging ODTs and, thus, pressure-induced miscibility.

The use of sustainable feedstocks extends beyond biomass to include CO_2, utilizing the product of carbon capture which will only become more available in coming years as carbon capture technologies advance. By using CO_2 as a feedstock for polymer synthesis, baroplastics can contribute to reducing atmospheric CO_2 levels, addressing both plastic waste and greenhouse gas emissions simultaneously [126]. In their 2022 study, Taniguchi et al. reported the baroplastic behavior of DBCPs of poly(trimethylene carbonate) (PTMC) with PLLA or poly(D-lactide) (PDLA) synthesized by ROP [15]. Here, both the PLA hard-blocks and the PTMC soft-blocks can be derived from renewable resources, with a recent study having prepared the monomer required for PTMC, trimethylene carbonate (TMC), from bio-based 1,3-propanediol and CO_2 [127]. Notably, PTMC is not an aliphatic polyester, but an aliphatic polycarbonate. Structurally similar to aliphatic polyesters, aliphatic polycarbonates show slower rates of biodegradation, opening up potential to tune the lifetime of a material in a specific natural environment by combining polyesters and polycarbonate [128]. Initially, the polymer pair was predicted to exhibit baroplastic behavior according to modelling with the CRS equation (Eq. (1)). The authors then identified a suitable range for hard-segment PLA content, w_{hard} = 33–57 wt% with an M_w of 34–100 kDa, that allowed for effective processing at 25 °C and 30 MPa. Increases to both the weight fraction of PLA and the MW of the DBCP gave higher minimum processing temperatures of 36–95 °C. Reducing the applied pressure increased the temperature required for processing, with the temperature required for processing a PLLA-*b*-PTMC DBCP with a w_{hard} of 48 wt% and a M_w of 45 kDa increasing from 40 °C at 49 MPa to 80 °C at 9 MPa. That DBCP was then reprocessed 10 times at 70 °C and 49 MPa, with no significant changes to its melt flow rate, Young's modulus, or tensile strength. As a control, a single high-temperature processing cycle was conducted at 200 °C, which showed a MW reduction of over 5 %, far greater than the insignificant changes caused by multiple 70 °C baroplastic processing cycles.

Unlike those mentioned in Section 3.3, the articles concerning sustainable polyester and polycarbonate BCPs focused heavily on mechanical properties, which can be more easily interpreted and reproduced, when compared with techniques such as AFM, TEM, SAXS, or SANS. Clearly, these materials have progressed far closer to real-life applications, and it simply remains to be seen if the mechanical properties can be increased further to offer a genuine alternative to some commercial polymers. Natural polysaccharides, such as starch can act as a source of glucose for the production of monomers required for both PLAs and PTMC, leveraging renewable resources and integrating carbon capture into the material's lifecycle. Any polymer lost throughout the baroplastic recycling process biodegrades into CO_2 and water in the natural environment, demonstrating the circular economic lifetime of baroplastics. By replacing petrochemical-derived monomers, the overall dependence on fossil fuels is reduced. This shift not only decreases greenhouse gas emissions but also conserves finite natural resources. Thinking into the future, this opens doors for future research into the development of new monomers from renewable feedstocks that, when

copolymerized, exhibit baroplastic behavior. Additionally, the combination of aliphatic polyesters and polycarbonates, which exhibit different rates of hydrolysis, may open the door to highly-tuneable rates of biodegradation, which can be tweaked for specific applications.

6. Conclusions and outlook

Despite flying under the radar of most polymer chemists, the field of baroplastics has continuously advanced over the past two decades. Analogous low-temperature processability has been demonstrated in Polymer Blends, BCPs, and CSNPs derived from both petrochemical and sustainable feedstocks. In this review, we have discussed all existing baroplastic literature in detail, which brings the ever-progressing nature of the research area into sharp focus. Baroplastics have been demonstrated to offer a number of tangible benefits over conventional thermoplastics: in particular their ability to be recycled multiple times without property degradation and their ability to incorporate thermally-sensitive components within nanocomposites. These, combined with the potential to incorporate a variety of functionalities and the compatibility with bio-based and/or bio-degradable polymer types, provide a strong case for the usage of baroplastics in a number of applications.

Further extensive research in the field of baroplastic materials has the potential to revolutionize how we approach the area of sustainable plastics through the introduction of a solution in parallel with the circular-economy model. Moreover, the added advantage of multiple processing cycles without thermo-oxidative side reactions results in a favorable elongated polymer lifetime and reduced long-term expenditure for manufacturers. When also derived from renewable sources, baroplastic materials can become an alternative to petroleum-based thermoplastics while simultaneously making them suitable candidates for several biomedical materials due to their low temperature formability. Despite the name 'baroplastics' being first reported over 20 years ago, in 2003, this review has demonstrated the tremendous scope for fundamental research within this relatively new field of polymer science. The majority of baroplastic work has focused on BCPs and CSNPs. While CSNPs are simpler to synthesize, they may irreversibly form macro-phase separated polymer blends if heated above the T_g of the hard segment (Typically ≈100 °C). Therefore, a pragmatic approach to the development of new baroplastic polymer pairs may be to first screen materials with easily-synthesized CSNPs, before switching to BCPs for specific polymer pairs of interest. There is significant potential to exploit polymer architectures, looking into graft and branched copolymers, BCPs with >2 blocks, as well as novel monomer combinations and MW distributions. Notably, the balance between a material's mechanical properties and ease of processability remains a critical factor in identifying original baroplastic polymer pairs. As a result, it is paramount that more research is undertaken in exploring the molecular mechanisms that determine ODT transitions to better understand and exploit these materials potential. While this review aims to inspire future developments of novel baroplastics, it also heavily emphasizes the importance of leveraging the pressure-responsive properties of baroplastics for novel applications within adhesives, lubricants, medical grade packaging, and sensors. There are a lot of stones left unturned within the field of baroplastics: while this presents a significant challenge for future researchers, there exists the potential to help solve enormous global problems.

Declaration of competing interest

The authors declare no conflicting interest.

CRediT authorship contribution statement

Daniel MacKinnon: Writing – review & editing. **Magdalena Godzina:** Writing – original draft. **C. Remzi Becer:** Writing – review & editing.

Data availability

No data was used for the research described in the article.

References

[1] Meng F, Brandão M, Cullen JM. Replacing plastics with alternatives is worse for greenhouse gas emissions in most cases. Environ Sci Technol 2024;58:2716–27. doi:10.1021/acs.est.3c05191.
[2] Geyer R, Jambeck JR, Law KL. Production, use, and fate of all plastics ever made. Sci Adv 2017;3:e1700782 -e. doi:10.1126/sciadv.1700782.
[3] Schneiderman DK, Hillmyer MA. 50th anniversary perspective: there is a great future in sustainable polymers. Macromolecules 2017;50:3733–49. doi:10.1021/acs.macromol.7b00293.
[4] Cabernard L, Pfister S, Oberschelp C, Hellweg S. Growing environmental footprint of plastics driven by coal combustion. Nat Sustain 2022;5:139–48. doi:10.1038/s41893-021-00807-2.
[5] UNEP How the world can end plastic pollution and create a circular economy Turning off the tap. United Nations Environment Programme; 2023 https://www.unep.org/resources/turning-off-tap-end-plastic-pollution-create-circular-economy (accessed 20/11/2024).
[6] Jehanno C, Alty JW, Roosen M, De Meester S, Dove AP, Chen EY X, et al. Critical advances and future opportunities in upcycling commodity polymers. Nat 2022;603:803–14. doi:10.1038/s41586-021-04350-0.
[7] Vidal F, van der Marel E R, Kerr RW F, McElroy C, Schroeder N, Mitchell C, et al. Designing a circular carbon and plastics economy for a sustainable future. Nat 2024;626:45–57. doi:10.1038/s41586-023-06939-z.
[8] Singh S, Ru J. Goals of sustainable infrastructure, industry, and innovation: a review and future agenda for research. ESPR 2023;30:28446–58. doi:10.1007/s11356-023-25281-5.
[9] OECD. Global plastics outlook: policy scenarios to 2060; Paris. https://doi.org/10.1787/aa1edf33-en, 2022, +.
[10] Directive EU. 904 of the european parliament and of the council of 5 june 2019 on the reduction of the impact of certain plastic products on the environment. Off J Eur Union 2019.
[11] European C. A new circular economy action plan for a cleaner and more competitive europe. Belgium: European Commission: Brussels; 2020. p. 1–20.
[12] Foschi E, Bonoli A. The commitment of packaging industry in the framework of the european strategy for plastics in a circular economy. Adm Sci 2019;9:18.
[13] Burgess M, Holmes H, Sharmina M, Shaver MP. The future of uk plastics recycling: one bin to rule them all. Resour Conserv Recycl 2021;164:105191. doi:10.1016/j.resconrec.2020.105191.
[14] Gonzalez-Leon JA, Acar MH, Ryu S-W, Ruzette A-VG, Mayes AM. Low-temperature processing of 'baroplastics' by pressure-induced flow. Nat 2003;426:424–8. doi:10.1038/nature02140.
[15] Taniguchi I, Nguyen TT T, Kinugasa K, Masutani K. A strategy to enhance recyclability of degradable block copolymers by introducing low-temperature formability. J Mater Chem A 2022;10:25446–52. doi:10.1039/D2TA06036A.
[16] Taniguchi I, Lovell NG. Low-temperature processable degradable polyesters. Macromolecules 2012;45:7420–8. doi:10.1021/ma301230y.
[17] Degaki H, Taniguchi I, Deguchi S, Koga T. Critical role of lattice vacancies in pressure-induced phase transitions of baroplastic diblock copolymers. Soft Matter 2024. doi:10.1039/D4SM00098F2025.
[18] Russell TP, Karis TE, Gallot Y, Mayes AM. A lower critical ordering transition in a diblock copolymer melt. Nat 1994;368:729–31. doi:10.1038/368729a0.
[19] Ruzette A-V. Copolymers close the loop. Nat Mater 2002;1:85–7. doi:10.1038/nmat739.
[20] Ruzette A-VG, Mayes AM. A simple free energy model for weakly interacting polymer blends. Macromolecules 2001;34:1894–907 +. doi:10.1021/ma000712.
[21] Ruzette AV G, Banerjee P, Mayes AM, Russell TP. A simple model for baroplastic behavior in block copolymer melts. J Chem Phys 2001;114:8205–9. doi:10.1063/1.1361072.
[22] Ruzette AV G, Mayes AM, Pollard M, Russell TP, Hammouda B. Pressure effects on the phase behavior of styrene/n-alkyl methacrylate block copolymers. Macromolecules 2003;36:3351–6. doi:10.1021/ma021394c.
[23] Ryu DY, Park MS, Chae SH, Jang J, Kim JK, Russell TP. Phase behavior of polystyrene and poly(n-pentyl methacrylate) blend. Macromolecules 2002;35:8676–80. doi:10.1021/ma025615q.
[24] Yeol Ryu D, Jeong U, Kon Kim J, Russell TP. Closed-loop phase behaviour in block copolymers. Nat Mater 2002;1:114–17. doi:10.1038/nmat724.
[25] Lv Z, Qiao J-N, Song Y-N, Ji X, Tang J-H, Yan D-X, et al. Baroplastics with robust mechanical properties and reserved processability through hydrogen-bonded interactions. ACS Appl Mater Interfaces 2019;11:12008–16. doi:10.1021/acsami.8b20676.

[26] Qiao J-N, Yang Q-C, Li Y, lv Z, Tang J-H, Lei J, et al. Baroplastics with ultrahigh strength and modulus via hydrogen-bonding interactions with agar. ACS Appl Polym Mater 2020;2:5550–7. doi:10.1021/acsapm.0c00892.
[27] Hewlett SA. Incorporation of silica into baroplastic core-shell nanoparticles. Massachusetts Institute of Technology; 2006. (accessed 17/11/2024).
[28] Iwasaki Y, Takemoto K, Tanaka S, Taniguchi I. Low-temperature processable block copolymers that preserve the function of blended proteins. Biomacromolecules 2016;17:2466–71. doi:10.1021/acs.biomac.6b00641.
[29] Lv Z, Jia C-L, Ji X, Yan D-X, Lei J, Repeatable Li Z-M. room-temperature-processed baroplastic-carbon nanotube composites for electromagnetic interference shielding. J Mater Chem C 2018;6:12955–64. doi:10.1039/C8TC04348E.
[30] Qiao J-N, Hu Y-F, Ji X, Tang J-H, Lei J, Li Z-M. Room-temperature repeatedly processable baroplastic/boron nitride thermal management composite. J Mater Chem C 2021;9:10388–97. doi:10.1039/D1TC01996A.
[31] Tang W, C-e He, Wang Y, Yang Y, Tsui CP. Low-temperature baroplastic processing of graphene-based polymer composites by pressure-induced flow. IOP Conf Ser: Mater Sci Eng 2014;62:012023.
[32] Xu Y, Brittain WJ, Vaia RA, Price G. Improving the physical properties of pea/pmma blends by the uniform dispersion of clay platelets. Polym 2006;47:4564–70. doi:10.1016/j.polymer.2006.03.108.
[33] Gonzalez-Leon JA, Mayes AM. Phase behavior prediction of ternary polymer mixtures. Macromolecules 2003;36:2508–15. doi:10.1021/ma0209803.
[34] Pollard M, Russell TP, Ruzette AV, Mayes AM, Gallot Y. The effect of hydrostatic pressure on the lower critical ordering transition in diblock copolymers. Macromolecules 1998;31:6493–8. doi:10.1021/ma980316f.
[35] Ruzette AV G, Banerjee P, Mayes AM, Pollard M, Russell TP, Jerome R, et al. Phase behavior of diblock copolymers between styrene and n-alkyl methacrylates. Macromolecules 1998;31:8509–16. doi:10.1021/ma981055c.
[36] Russell TP, Lee DH. Performing under pressure. Nat Nanotech 2009;4:703–4. doi:10.1038/nnano.2009.328.
[37] Paul DR, Barlow JW. Polymer blends. J Macromol Sci C 1980;18:109–68. doi:10.1080/00222358008080917.
[38] Alkhodairi H, Russell ST, Pribyl J, Benicewicz BC, Kumar SK. Compatibilizing immiscible polymer blends with sparsely grafted nanoparticles. Macromolecules 2020;53:10330–8. doi:10.1021/acs.macromol.0c02108.
[39] Han CD, Kim J, Kim JK, Chu SG. Viscoelastic behavior of mixtures of a block copolymer and a homopolymer. Macromolecules 1989;22:3443–51.
[40] Harada A, Furue M, Nozakura S-i. Cyclodextrin-containing polymers. 1. Preparation of polymers. Macromolecules 1976;9:701–4.
[41] Shinitzky M. Effect of fluorescence polarization on fluorescence intensity and decay measurements. J Chem Phys 1972;56:5979–81.
[42] Bernstein RE, Cruz CA, Paul DR, Barlow JW. Lcst behavior in polymer blends. Macromolecules 1977;10:681–6.
[43] Karis TE, Russell TP, Gallot Y, Mayes AM. Rheology of the lower critical ordering transition. Macromolecules 1995;28:1129–34.
[44] Boudouris D, Constantinou L, Panayiotou C. A group contribution estimation of the thermodynamic properties of polymers. Ind Eng Chem Res 1997;36:3968–73. doi:10.1021/ie970242g.
[45] Olabisi O, Simha R. Pressure-volume-temperature studies of amorphous and crystallizable polymers. I. Experimental. Macromolecules 1975;8:206–10. doi:10.1021/ma60044a022.
[46] Quach A, Simha R. Pressure-volume-temperature properties and transitions of amorphous polymers; polystyrene and poly (orthomethylstyrene). J Appl Phys 1971;42:4592–606. doi:10.1063/1.1659828.
[47] Hammouda B, Bauer BJ. Compressibility of two polymer blend mixtures. Macromolecules 1995;28:4505–8. doi:10.1021/ma00117a019.
[48] Janssen S, Schwahn D, Mortensen K, Springer T. Pressure dependence of the flory-huggins interaction parameter in polymer blends: a sans study and a comparison to the flory-orwoll-vrij equation of state. Macromolecules 1993;26:5587–91. doi:10.1021/ma00073a009.
[49] Flory PJ. Principles of polymer chemistry. New York: Cornell university press; 1953.
[50] Hasegawa H, Sakamoto N, Takeno H, Jinnai H, Hashimoto T, Schwahn D, et al. Small-angle neutron scattering studies on phase behavior of block copolymers. J Phys Chem Solids 1999;60:1307–12. doi:10.1016/S0022-3697(99)00109-2.
[51] Rodgers PA. Pressure–volume–temperature relationships for polymeric liquids: a review of equations of state and their characteristic parameters for 56 polymers. J Appl Polym Sci 1993;48:1061–80.
[52] Freeman PI, Rowlinson JS. Lower critical points in polymer solutions. Polym 1960;1:20–6.
[53] Sanchez IC, Panayiotou CG. Equation of state. In: Models in thermodynamics and phase equilibria calculations. New York: Marcel Dekker; 1993. p. 187–286.
[54] Beiner M, Fytas G, Meier G, Kumar SK. Pressure-induced compatibility in a model polymer blend. PRL 1998;81:594–7. doi:10.1103/PhysRevLett.81.594.
[55] Lefebvre AA, Lee JH, Balsara NP, Hammouda B, Krishnamoorti R, Kumar S. Relationship between internal energy and volume change of mixing in pressurized polymer blends. Macromolecules 1999;32:5460–2.
[56] Flory PJ, Orwoll RA, Vrij A. Statistical thermodynamics of chain molecule liquids. Ii. Liquid mixtures of normal paraffin hydrocarbons. J Am Chem Soc 1964;86:3515–20. doi:10.1021/ja01071a024.
[57] Prigogine I, Bellemans A, Mathot V. The molecular theory of solutions. Amsterdam: North-Holland Publishing Company; 1957.
[58] Dudowicz J, Freed KF. Effect of monomer structure and compressibility on the properties of multicomponent polymer blends and solutions: 1. Lattice cluster theory of compressible systems. Macromolecules 1991;24:5076–95. doi:10.1021/ma00018a014.
[59] Lacombe RH, Sanchez IC. Statistical thermodynamics of fluid mixtures. J Phys Chem 1976;80:2568–80. doi:10.1021/j100564a009.
[60] McMaster LP. Aspects of polymer-polymer thermodynamics. Macromolecules 1973;6:760–73. doi:10.1021/ma60035a024.
[61] Callaghan TA, Paul DR. Interaction energies for blends of poly(methyl methacrylate), polystyrene, and poly(alpha.-methylstyrene) by the critical molecular weight method. Macromolecules 1993;26:2439–50. doi:10.1021/ma00062a008.
[62] Krevelen DW, Hoftyzer PJ. Properties of polymers: correlations with chemical structure. Oxford: Elsevier Publishing Company; 1972.
[63] Hudson CS. Die gegenseitige löslichkeit von nikotin in wasser. Z Phys Chem 1904;47:113–15.
[64] Bates FS, Wignall GD, Koehler WC. Critical behavior of binary liquid mixtures of deuterated and protonated polymers. PRL 1985;55:2425–8. doi:10.1103/PhysRevLett.55.2425.
[65] Dorigato A, Fredi G. Effect of nanofillers addition on the compatibilization of polymer blends. Adv Ind Eng Polym Res 2023. doi:10.1016/j.aiepr.2023.09.004.
[66] Fornes TD, Yoon PJ, Paul DR. Polymer matrix degradation and color formation in melt processed nylon 6/clay nanocomposites. Polym 2003;44:7545–56. doi:10.1016/j.polymer.2003.09.034.
[67] Clark EA, Lipson JE G. Lcst and ucst behavior in polymer solutions and blends. Polym 2012;53:536–45. doi:10.1016/j.polymer.2011.11.045.
[68] Ougizawa T, Inoue T. Ucst and lcst behavior in polymer blends and its thermodynamic interpretation. Polym J 1986;18:521–7. doi:10.1295/polymj.18.521.
[69] Lee K-H, Ryu S-W. Room temperature baroplastic processing of ps/pba nano-blends. Macromol Res 2012;20:1294–9. doi:10.1007/s13233-012-0186-z.
[70] Leibler L. Theory of microphase separation in block copolymers. Macromolecules 1980;13:1602–17. doi:10.1021/ma60078a047.
[71] Ruzette A-VG. Molecular design of ordering transitions in block copolymers. Massachusetts Institute of Technology; 2000. (accessed 14/11/2024).
[72] Ahn H, Lee Y, Lee H, Han YS, Seong BS, Ryu DY. Various phase behaviors of weakly interacting binary block copolymer blends. Macromolecules 2013;46:4454–61. doi:10.1021/ma302514s.
[73] Jo A, Gu GH, Moon HC, Han SH, Oh SH, Park CG, et al. In situ tem observation of phase transition of the nanoscopic patterns on baroplastic block copolymer films during nanoindentation. Nanoscale 2013;5:4351–4. doi:10.1039/C3NR00447C.
[74] Lee DH, Kim HJ, Kim JK. Closed-loop phase behavior and baroplasticity of deuterated polystyrene-block-poly(n-pentyl methacrylate) copolymer investigated by sans and ftir spectroscopy. Macromol Symp 2006;240:123–9. doi:10.1002/masy.200650816.
[75] Ryu DY, Lee DJ, Kim JK, Lavery KA, Russell TP, Han YS, et al. Effect of hydrostatic pressure on closed-loop phase behavior of block copolymers. PRL 2003;90:235501. doi:10.1103/PhysRevLett.90.235501.
[76] Qian C, Mumby SJ, Eichinger BE. Phase diagrams of binary polymer solutions and blends. Macromolecules 1991;24:1655–61. doi:10.1021/ma00007a031.
[77] Jo A, Joo W, Jin W-H, Nam H, Kim JK. Ultrahigh-density phase-change data storage without the use of heating. Nat Nanotech 2009;4:727–31. doi:10.1038/nnano.2009.260.
[78] Kim HJ, Moon HC, Kim H, Kim K, Kim JK, Cho J. Pressure effect of various inert gases on the phase behavior of polystyrene-block-poly(n-pentyl methacrylate) copolymer. Macromolecules 2013;46:493–9. doi:10.1021/ma302155j.
[79] Walker TA, Frankowski DJ, Spontak RJ. Thermodynamics and kinetic processes of polymer blends and block copolymers in the presence of pressurized carbon dioxide. Adv Mater 2008;20:879–98. doi:10.1002/adma.200700076.
[80] Mok MM, Ellison CJ, Torkelson JM. Effect of gradient sequencing on copolymer order–disorder transitions: phase behavior of styrene/n-butyl acrylate block and gradient copolymers. Macromolecules 2011;44:6220–6. doi:10.1021/ma201080n.
[81] Lefebvre MD, Olvera de la Cruz M, Shull KR. Phase segregation in gradient copolymer melts. Macromolecules 2004;37:1118–23. doi:10.1021/ma035141a.
[82] Lee Y, Lee H, Kim S-W, Park S, Kim E, Han YS, et al. Baroplastic behavior of miscible block copolymer blends. Polym 2014;55:6967–72. doi:10.1016/j.polymer.2014.11.011.
[83] Ghosh Chaudhuri R, Paria S. Core/shell nanoparticles: classes, properties, synthesis mechanisms, characterization, and applications. Chem Rev 2012;112:2373–433. doi:10.1021/cr100449n.
[84] Gonzalez-Leon JA, Ryu S-W, Hewlett SA, Ibrahim SH, Mayes AM. Core–shell polymer nanoparticles for baroplastic processing. Macromolecules 2005;38:8036–44. doi:10.1021/ma0508045.
[85] Hourston DJ, Song M, Hammiche A, Pollock HM, Reading M. Modulated differential scanning calorimetry: 6. Thermal characterization of multicomponent polymers and interfaces. Polym 1997;38:1–7. doi:10.1016/S0032-3861(96)00466-1.
[86] Song M, Hammiche A, Pollock HM, Hourston DJ, Reading M. Modulated differential scanning calorimetry: 1. A study of the glass transition behaviour of blends of poly(methyl methacrylate) and poly(styrene-co-acrylonitrile). Polym 1995;36:3313–16. doi:10.1016/0032-3861(95)99430-3.

[87] Stubbs JM, Sundberg DC. A round robin study for the characterization of latex particle morphology—Multiple analytical techniques to probe specific structural features. Polym 2005;46:1125–38. doi:10.1016/j.polymer.2004.11.079.
[88] Sundberg DC, Durant YG. Latex particle morphology, fundamental aspects: a review. Polym React Eng 2003;11:379–432. doi:10.1081/PRE-120024420.
[89] Flemings MC. Behavior of metal alloys in the semisolid state. Metall Mater Trans B 1991;22:269–93. doi:10.1007/BF02651227.
[90] Ballauff M, Wolf BA. Degradation of chain molecules. 1. Exact solution of the kinetic equations. Macromolecules 1981;14:654–8. doi:10.1021/ma50004a039.
[91] Buchholz BA, Zahn JM, Kenward M, Slater GW, Barron AE. Flow-induced chain scission as a physical route to narrowly distributed, high molar mass polymers. Polym 2004;45:1223–34. doi:10.1016/j.polymer.2003.11.051.
[92] Merrill EW, Leopairat P. Scission of non-interpenetrating macromolecules in transient extensional flows. Polym Eng Sci 1980;20:505–11. doi:10.1002/pen.760200711.
[93] Metzner AB, Metzner AP. Stress levels in rapid extensional flows of polymeric fluids. Rheol Acta 1970;9:174–81. doi:10.1007/BF01973476.
[94] Bonetti S, Farina M, Mauri M, Koynov K, Butt H-J, Kappl M, et al. Core@shell poly(n-butylacrylate)@polystyrene nanoparticles: baroplastic force-responsiveness in presence of strong phase separation. Macromol Rapid Commun 2016;37:584–9. doi:10.1002/marc.201500625.
[95] An N, Wang X, Li Y, Zhang L, Lu Z, Sun J. Healable and mechanically superstrong polymeric composites derived from hydrogen-bonded polymeric complexes. Adv Mater 2019;31:1904882. doi:10.1002/adma.201904882.
[96] An N, Zhu Y, Wang X, Li Y, Liu J, Fang X, et al. Dual nanofillers-reinforced noncovalently cross-linked polymeric composites with unprecedented mechanical strength. CCS Chemistry 2023;5:2312–23. doi:10.31635/ccschem.022.202202496.
[97] Kloxin CJ, Bowman CN. Covalent adaptable networks: smart, reconfigurable and responsive network systems. Chem Soc Rev 2013;42:7161–73. doi:10.1039/c3cs60046g.
[98] Chen Q, Zhu L, Zhao C, Wang Q, Zheng J. A robust, one-pot synthesis of highly mechanical and recoverable double network hydrogels using thermoreversible sol-gel polysaccharide. Adv Mater 2013;25:4171–6. doi:10.1002/adma.201300817.
[99] Feng Z, Zuo H, Gao W, Ning N, Tian M, Zhang L. A robust, self-healable, and shape memory supramolecular hydrogel by multiple hydrogen bonding interactions. Macromol Rapid Commun 2018;39:1800138. doi:10.1002/marc.201800138.
[100] Li X, Yang Q, Zhao Y, Long S, Zheng J. Dual physically crosslinked double network hydrogels with high toughness and self-healing properties. Soft Matter 2017;13:911–20. doi:10.1039/C6SM02567F.
[101] Normand V, Lootens DL, Amici E, Plucknett KP, Aymard P. New insight into agarose gel mechanical properties. Biomacromolecules 2000;1:730–8. doi:10.1021/bm005583j.
[102] Xiong J-Y, Narayanan J, Liu X-Y, Chong TK, Chen SB, Chung T-S. Topology evolution and gelation mechanism of agarose gel. J Phys Chem B 2005;109:5638–43. doi:10.1021/jp044473u.
[103] Liu J, Tan CS Y, Yu Z, Li N, Abell C, Scherman OA. Tough supramolecular polymer networks with extreme stretchability and fast room-temperature self-healing. Adv Mater 2017;29:1605325. doi:10.1002/adma.201605325.
[104] Verjans J, André A, Sedlačík T, Aksakal R, van Ruymbeke E, Hoogenboom R. Physically crosslinked polyacrylates by quadruple hydrogen bonding side chains. J Mater Chem B 2024;12:12378–89. doi:10.1039/D4TB01702A.
[105] Chen S, Sun L, Zhou X, Guo Y, Song J, Qian S, et al. Mechanically and biologically skin-like elastomers for bio-integrated electronics. Nat Commun 2020;11:1107. doi:10.1038/s41467-020-14446-2.
[106] Whitesides GM. Soft robotics. Angew Chem Int Ed 2018;57:4258–73. doi:10.1002/anie.201800907.
[107] Kloxin CJ, Scott TF, Adzima BJ, Bowman CN. Covalent adaptable networks (cans): a unique paradigm in crosslinked polymers. Macromolecules 2010;43:2643–53. doi:10.1021/ma902596s.
[108] Canary SA, Stevens MP. Thermally reversible crosslinking of polystyrene via the furan–maleimide diels–alder reaction. J Polym Sci A: Polym Chem 1992;30:1755–60. doi:10.1002/pola.1992.080300829.
[109] Canadell J, Goossens H, Klumperman B. Self-healing materials based on disulfide links. Macromolecules 2011;44:2536–41. doi:10.1021/ma2001492.
[110] Deng CC, Brooks WL A, Abboud KA, Sumerlin BS. Boronic acid-based hydrogels undergo self-healing at neutral and acidic ph. ACS Macro Lett 2015;4:220–4. doi:10.1021/acsmacrolett.5b00018.
[111] Zydziak N, Yameen B, Barner-Kowollik C. Diels–alder reactions for carbon material synthesis and surface functionalization. Polym Chem 2013;4:4072–86. doi:10.1039/C3PY00232B.
[112] MacKinnon DJ, Drain B, Becer CR. Exploring polymeric diene–dienophile pairs for thermoreversible diels–alder reactions. Macromolecules 2024;57:6024–34. doi:10.1021/acs.macromol.4c00832.
[113] Tada H, Taniguchi I. Pressure-induced formability and degradability of block copolymers composed of poly(1,5-dioxepan-2-one) and poly(l-lactide). Polym Deg Stab 2024;230:111048. doi:10.1016/j.polymdegradstab.2024.111048.
[114] Lovell NG. The design, synthesis and properties of pressure-processable biodegradable block copolymers. Massachusetts Institute of Technology; 2005. (accessed 22/11/2024).
[115] PlasticsEurope Plastics – the fast facts 2023; 2023 https://plasticseurope.org/knowledge-hub/plastics-the-fast-facts-2023/ (accessed 20/11/2024).
[116] Hayes G, Laurel M, MacKinnon D, Zhao T, Houck HA, Becer CR. Polymers without petrochemicals: sustainable routes to conventional monomers. Chem Rev 2023;123:2609–734. doi:10.1021/acs.chemrev.2c00354.
[117] Zhu Y, Romain C, Williams CK. Sustainable polymers from renewable resources. Nat 2016;540:354–62. doi:10.1038/nature21001.
[118] Babu RP, O'Connor K, Seeram R. Current progress on bio-based polymers and their future trends. Prog Biomater 2013;2:8. doi:10.1186/2194-0517-2-8.
[119] Nakajima H, Dijkstra P, Loos K. The recent developments in biobased polymers toward general and engineering applications: polymers that are upgraded from biodegradable polymers, analogous to petroleum-derived polymers, and newly developed. Polymers (Basel) 2017;9:523. doi:10.3390/polym9100523.
[120] Lim LT, Auras R, Rubino M. Processing technologies for poly(lactic acid). Prog Polym Sci 2008;33:820–52. doi:10.1016/j.progpolymsci.2008.05.004.
[121] Montaudo G, Puglisi C, Samperi F. Primary thermal degradation mechanisms of pet and pbt. Polym Deg Stab 1993;42:13–28. doi:10.1016/0141-3910(93)90021-A.
[122] Deguchi S, Degaki H, Taniguchi I, Koga T. Deep-sea-inspired chemistry: a hitchhiker's guide to the bottom of the ocean for chemists. Langmuir 2023;39:7987–94. doi:10.1021/acs.langmuir.3c00516.
[123] Williams CK. Synthesis of functionalized biodegradable polyesters. Chem Soc Rev 2007;36:1573–80. doi:10.1039/B614342N.
[124] Vert M. Aliphatic polyesters: Great degradable polymers that cannot do everything. Biomacromolecules 2005;6:538–46. doi:10.1021/bm0494702.
[125] Buntara T, Noel S, Phua PH, Melián-Cabrera I, de Vries JG, Heeres HJ. Caprolactam from renewable resources: catalytic conversion of 5-hydroxymethylfurfural into caprolactone. Angew Chem Int Ed 2011;50:7083–7. doi:10.1002/anie.201102156.
[126] Hepburn C, Adlen E, Beddington J, Carter EA, Fuss S, Mac Dowell N, et al. The technological and economic prospects for co2 utilization and removal. Nat 2019;575:87–97. doi:10.1038/s41586-019-1681-6.
[127] Honda M, Tamura M, Nakao K, Suzuki K, Nakagawa Y, Tomishige K. Direct cyclic carbonate synthesis from co2 and diol over carboxylation/hydration cascade catalyst of ceo2 with 2-cyanopyridine. ACS Catal 2014;4:1893–6. doi:10.1021/cs500301d.
[128] Yu W, Maynard E, Chiaradia V, Arno MC, Dove AP. Aliphatic polycarbonates from cyclic carbonate monomers and their application as biomaterials. Chem Rev 2021;121:10865–907. doi:10.1021/acs.chemrev.0c00883.